

South Dakota State University

## Open PRAIRIE: Open Public Research Access Institutional Repository and Information Exchange

---

Electronic Theses and Dissertations

---

1961

### Some Electrical Characteristics of C3F8 Electrode Systems

Yarlagadda Radha Krishna Rao

Follow this and additional works at: <https://openprairie.sdstate.edu/etd>

---

#### Recommended Citation

Rao, Yarlagadda Radha Krishna, "Some Electrical Characteristics of C3F8 Electrode Systems" (1961). *Electronic Theses and Dissertations*. 2791.  
<https://openprairie.sdstate.edu/etd/2791>

This Thesis - Open Access is brought to you for free and open access by Open PRAIRIE: Open Public Research Access Institutional Repository and Information Exchange. It has been accepted for inclusion in Electronic Theses and Dissertations by an authorized administrator of Open PRAIRIE: Open Public Research Access Institutional Repository and Information Exchange. For more information, please contact [michael.biondo@sdstate.edu](mailto:michael.biondo@sdstate.edu).

39

**SOME ELECTRICAL CHARACTERISTICS OF  $C_3F_8$  AND  
AIR WITH VARIOUS ELECTRODE SYSTEMS**

**BY**

**YARLAGADDA RADHA KRISHNA RAO**

**A thesis submitted  
in partial fulfillment of the requirements for the  
degree Master of Science, Department of  
Electrical Engineering, South Dakota  
State College of Agriculture  
and Mechanic Arts**

**December 1961**

**SOUTH DAKOTA STATE COLLEGE LIBRARY**



26610

**SOME ELECTRICAL CHARACTERISTICS OF  $C_3F_8$  AND  
AIR WITH VARIOUS ELECTRODE SYSTEMS**

This thesis is approved as a creditable, independent investigation by a candidate for the degree, Master of Science, and is acceptable as meeting the thesis requirements for this degree, but without implying that the conclusions reached by the candidate are necessarily the conclusions of the major department.

\_\_\_\_\_  
Thesis Adviser

\_\_\_\_\_  
Head of the Major Department

## ACKNOWLEDGMENT

The author wishes to express his sincere appreciation towards Dr. Kenneth E. Lindley for suggesting the problem and for his guidance, help, and encouragement given in these experiments, as well as in writing the thesis. The help given by him during the course work is especially appreciated.

The author also wishes to express his sincere appreciation to Dean M. L. Manning for allowing him the use of his library and his great encouragement in research in this area at South Dakota State College.

The author wishes to express his gratitude towards Dr. Lindley and Professor Perry Williams for allowing him to use their equipment during these experiments.

Special acknowledgments are also made to Professor William H. Gamble, Dr. Warren O. Essler, and other staff members for the help given by them during the stay of the author at State College.

The author also wishes to express his appreciation to Emmy E. Brown for typing the thesis.

YRKR

## TABLE OF CONTENTS

Chapter	Page
I. INTRODUCTION . . . . .	1
II. REVIEW OF LITERATURE . . . . .	3
III. METHODS AND MATERIALS . . . . .	17
IV. BASIC THEORY . . . . .	21
A. <u>General Discussion</u> . . . . .	21
B. <u>Field Mapping</u> . . . . .	29
<u>General principles of field mapping, line, and</u> <u>tubes of force</u> . . . . .	30
<u>Equipotential surfaces</u> . . . . .	30
<u>Procedure in mapping</u> . . . . .	32
<u>Laws to be observed for the flow of flux</u> . . . . .	32
<u>Solution of one, two, and three dimensional fields</u>	32
C. <u>General Discussion of the Gases Used in These</u> <u>Experiments</u> . . . . .	41
D. <u>Breakdown of Gases Considering the Electrode</u> <u>Configuration</u> . . . . .	48
V. RESULTS AND DISCUSSION . . . . .	50
A. <u>Systems Used in Tests</u> . . . . .	50
<u>3/4" diameter sphere to 1 3/4" diameter plane</u> . .	50
<u>Point to 1 3/4" diameter plane</u> . . . . .	52
<u>Point to point</u> . . . . .	55
<u>1" diameter sphere to 1" square plane, superimposed</u> <u>on a 1 3/4" diameter plate</u> . . . . .	55

## TABLE OF CONTENTS (Continued)

Chapter	Page
3/4" square plane to 3/4" square plane . . . . .	58
1/2" square plane to 1 3/4" diameter plane . . .	61
<u>Comparison of discharges with various types of</u> <u>electrode systems</u> . . . . .	63
VI. CONCLUSIONS . . . . .	72
LITERATURE CITED . . . . .	73

## LIST OF FIGURES

Figure	Page
I. Gas control equipment . . . . .	18
II. Field map of a sphere to plane electrode system . . . .	37
III. Field map of a point to plane electrode system . . . .	38
IV. Field map of a point to point electrode system . . . .	39
V. Field map of a sphere to square plane, superimposed on a circular plane electrode system . . . . .	40
VI. Field map of a square plane to square plane (uncrossed) electrode system . . . . .	42
VII. Field map of a square plane to square plane (crossed) electrode system . . . . .	43
VIII. Field map of a square plane to circular plane electrode system . . . . .	44
IX. Breakdown strengths of $C_3F_8$ and air with the sphere to plane electrode system . . . . .	51
X. Breakdown strengths of $C_3F_8$ and air with the point to plane electrode system . . . . .	53
XI. Breakdown strengths of $C_3F_8$ and air with the point to point electrode system . . . . .	56
XII. Breakdown strengths of $C_3F_8$ and air with the sphere to square plane, superimposed on a circular plane electrode system . . . . .	57
XIII. Breakdown strengths of $C_3F_8$ and air with square plane to square plane (uncrossed) electrode system . . . . .	59
XIV. Breakdown strengths of $C_3F_8$ and air with square plane to square plane (crossed) electrode system . . . . .	60
XV. Breakdown strengths of $C_3F_8$ and air with square plane to circular plane electrode system . . . . .	62
XVI. Comparative study of breakdown strength of $C_3F_8$ with the electrode systems . . . . .	64

## LIST OF FIGURES (Continued)

Figure		Page
XVII.	Comparative study of breakdown strength of air with the electrode systems . . . . .	65
XVIII.	Pictures of the corona bursts observed on the oscilloscope with the following in the test cell . . .	67
	A - $C_3F_8$ with the sphere to plane electrode system	
	B - Air with the sphere to plane electrode system	
	C - $C_3F_8$ with the point to plane electrode system	
	D - Air with the point to plane electrode system	
XIX.	Pictures of the corona bursts observed on the oscilloscope with the following in the test cell . . .	68
	A - $C_3F_8$ with the point to point electrode system	
	B - $C_3F_8$ with the sphere to square plane, superimposed on a circular plane electrode system	
	C - Air with the sphere to square plane, superimposed on a circular plane electrode system	
	D - $C_3F_8$ with the square plane to square plane (uncrossed) electrode system	
XX.	Pictures of the corona bursts observed on the oscilloscope with the following in the test cell . . .	69
	A - $C_3F_8$ with the square plane to square plane (crossed) electrode system	
	B - $C_3F_8$ with the square plane to circular plane electrode system with gap distance of 0.1"	
	C - $C_3F_8$ with the square plane to circular plane electrode system with gap distance of 0.2"	
	D - $C_3F_8$ with the square plane to circular plane electrode system with gap distance of 0.3"	
XXI.	Pictures of the corona bursts observed on the oscilloscope with the following in the test cell . . .	70
	A - $C_3F_8$ with the square plane to circular plane electrode system with gap distance of 0.4"	
	B - $C_3F_8$ with the square plane to circular plane electrode system with gap distance of 0.5"	
	C - Air with the square plane to circular plane electrode system with gap distance of 0.3"	
	D - Air with the square plane to circular plane electrode system with gap distance of 0.4"	

## LIST OF FIGURES (Continued)

Figure	Page
XXII. Picture of the corona bursts observed on the oscilloscope with the following in the test cell . . .	71
Air with the square plane to circular plane electrode system with gap distance of 0.5"	

## CHAPTER I

### INTRODUCTION

This paper treats with corona discharges at normal pressure and at room temperature in  $C_3F_8$  and air with the following electrode systems:  $3/4$ " diameter sphere to  $1\ 3/4$ " diameter plane, point to  $1\ 3/4$ " diameter plane, point to point,  $1$ " diameter sphere to  $1$ " square plane, superimposed on a  $1\ 3/4$ " diameter plate,  $3/4$ " square plane to  $3/4$ " square plane (crossed and uncrossed), and  $1/2$ " square plane to  $1\ 3/4$ " diameter plane. The main discussions are: breakdown strength of these gases, mechanism of breakdown, and field mapping with the electrode systems.

For transformers and circuit breakers, insulation is most important for designing purposes. For transformers, oil is used for cooling and insulating. For circuit breakers, oil or some gases can be used for the purpose of quenching the arc. For these purposes, if gases are used, they should have high dielectric strength, noninflammability, etc. This paper discusses the dielectric strength of two gases and the effect in breakdown KV with different electrode systems at various gap settings. Oscillographic patterns of corona bursts for various electrode systems for the two gases are shown. Field analysis is also studied as it gives the physical concept of the system when the initiations of breakdown are confined to a single region of field, such as coiledges, clamps, and other sharp-edged electrode systems.

Corona discharges are the transitory, faintly luminous, and audible glows which can be observed in a discharge gap, near the sparking



value. Breakdown value of the gas depends upon the dielectric strength of the gas. It also depends upon electrode configuration; that is, concentrations of the field.  $C_2F_6$  has high dielectric strength; mainly, due to the electronegativity of the gas. Air has less, as it is a mixture of gases.

## CHAPTER II

### REVIEW OF LITERATURE

In the literature, one can observe the inconsistency of the many test methods used with various gases and various electrode systems.

Gases used were argon, helium, nitrogen, air, oxygen, hydrogen, fluorides,  $\text{SF}_6$ , perfluorocarbon vapors, and their mixtures with hydrogen and with hydrocarbons.

Investigators used several types of electrode systems which were sphere to sphere (with varying diameters), sphere to rod, sphere to plane, plane to plane, point to plane (positive point and negative point), rod to sphere, rod to plane, rod to rod, linked toroids, square rods, and projected rods. Some of the investigations will be reviewed. Manning<sup>1</sup> investigated with gases  $\text{SF}_6$ , air,  $\text{C}_3\text{F}_8$ , and nitrogen. In these, he used four types of brass electrode systems which were sphere to plane, rod to plane, sphere to square projected rod, and square rod to brass rod, superimposed on a circular plate.

For the test cell, he gave the following features: (1) It should be economical in use of a small quantity of gas; (2) suitable for general use; (3) suitable up to 50 KV; (4) able to use at atmospheric pressure; and (5) useful in the primary screening of gases, relative to each other.

---

<sup>1</sup>M. L. Manning, "Experience With the AIEE Subcommittee Test Cell for Gaseous Insulation", AIEE Transactions, vol. 78, 1959, pt. 3, pp. 800-807.

His test data indicate for spacing of .25", rapidly applied voltage breakdown values for 3/4" sphere to plane are 55% higher for SF<sub>6</sub> and 30% higher for C<sub>3</sub>F<sub>8</sub> than for 1/2" square rod to plane values. For 60 cycle voltage, 1 minute with stand strength .25" gap, the values are 59% higher for SF<sub>6</sub> and 20% higher for C<sub>3</sub>F<sub>8</sub> in comparing a 3/4" diameter sphere to plane with a 1/2" square rod to plane.

He compared the electric strength of gases for a given electrode system, also using the sphere to plane. The electric strength of SF<sub>6</sub> and N<sub>2</sub> is greater than C<sub>3</sub>F<sub>8</sub> and air. With 1/2" square rod to ground plane, it is found that the electric strength of C<sub>3</sub>F<sub>8</sub> and air is greater than SF<sub>6</sub> and N<sub>2</sub>.

Camilli and Chapman<sup>2</sup> studied the breakdown phenomenon with gases N<sub>2</sub>, CF<sub>2</sub>Cl<sub>2</sub>, CF<sub>3</sub>Cl, CF<sub>4</sub>, CHClF<sub>2</sub>, CHF<sub>3</sub>, and SF<sub>6</sub>. The electrodes used were 1" diameter sphere as a bottom electrode, which was at earth potential, and either 1" diameter sphere or a tungsten rod as a top electrode. The tests were conducted up to 350 KV. To protect the cell from external flash, it was immersed in oil. The tests were conducted with pressures 0, 15, and 30 pounds of gauge pressure. They studied the behavior of breakdown strength with variation of gases in pressure and complex gases with point electrodes. A sharp electrode creates ionization and space charge, prior to breakdown, and causes impulse time lag. This prebreakdown space charge sometimes reduces the field gradient in the neighborhood of the sharp electrode to such an extent that

---

<sup>2</sup>G. Camilli and J. J. Chapman, "Gaseous Insulation for High Voltage Apparatus", AIEE Transaction, vol. 66, 1947, pp. 1463-1470.

the final breakdown value is raised considerably. Finally, as the pressure increases further, the breakdown value decreases until breakdown begins to occur without any preionization process. They explained that  $\text{SF}_6$  has superior qualities over freons in uniform and nonuniform fields. They concluded that  $\text{SF}_6$  increases its dielectric strength with increase of pressure. Its properties of noninflammability, stability at high temperatures, increase in dielectric strength with pressure, and no deposit of carbon during tests (unlike the freons), make it superior over other gases.

Camilli and Plump<sup>3</sup> discussed in their paper the dielectric strength of various fluorine compounds. They compared the strength of  $\text{N}_2$  and  $\text{CCl}_2\text{F}_2$  with oil. For obtaining 60 cycle strength equal to oil,  $\text{N}_2$  requires a pressure of 80 lbs/square inch and  $\text{CCl}_2\text{F}_2$  requires about 25 lbs/square inch. These were tested with 6.25 cm spheres spaced at 1 cm apart. In a uniform field, 60 cycle strength of  $\text{SF}_6$  is about 75% of oil and at 30 lbs absolute, it is 63%. For  $\text{CCl}_2\text{F}_2$ , at 45 lbs absolute, it is 90% oil strength and 77% at 30 lbs absolute.

In a nonuniform field, using a pointed tungsten rod and sphere, separated 1", the 60 cycle a-c strength of  $\text{SF}_6$  was at 45 lbs absolute, 114% of oil and using  $\text{CCl}_2\text{F}_2$ , it was only 40% of oil. They discussed the effect of temperature, pressure, and electrode metals.

The effect of temperature is almost negligible provided that the density of the gas is held constant.

---

<sup>3</sup>G. Camilli and R. E. Plump, "Fluorine Containing Gaseous Dielectrics", AIIE Transactions, vol. 72, 1953, pt. 1, pp. 93-102.

The corrosion after arcing is different on different metals. Aluminium was found more resistant than brass and steel is even less resistant than either one. They discussed about the theoretical aspects of gas dielectric strengths, electron negativity, electron affinity, ionization potential, and electron trapping.

Cobine<sup>4</sup> discussed in his paper about the thermal and electrical characteristics of helium and sulphur hexafluoride mixtures. In his experiments, he used a bell jar with sphere electrodes (not exactly spheres). He explained the way to obtain breakdown KV of a pure gas, when there are traces of impurities. His explanation for this is, when a breakdown takes place in a gas containing some electronegative impurities, these impurities quickly attach electrons, then as negative ions, they are swept out of the volume by the electric field. If the voltage is quickly reapplied so that insufficient time is available for new impurities to diffuse into the gap, the breakdown voltage will be that of the pure gas.

He has shown that an addition of relatively small amounts of SF<sub>6</sub> to helium will result in an electric strength greater than that of air or hydrogen. Thermal properties are as good as hydrogen. He recommended these mixtures for cooling and for an insulating medium for both static and rotating machines.

---

<sup>4</sup>J. D. Cobine, "Some Electrical and Thermal Characteristics of Helium and Sulphur Hexafluoride Mixtures", AIEE Transactions, vol. 74, 1955, pt. 1, pp. 318-321.

Camilli, Liao, and Plump<sup>5</sup> conducted several experiments about the dielectric behavior of some fluorogases and their mixtures. In these experiments, they used round edged plane to plane and 1/4" square rod to plane as electrode systems. They discussed about the higher breakdown KV for the rod to plane in large gap spacings and the converse is true for small spacings. The reason is, negative ions formed at the rod during negative voltage crest would be swept into the plane before the next half cycle, therefore, the breakdown can be indicated by a positive streamer. At large spacings, negative ions formed during the negative half cycle do not have time to be swept out completely and return to the rod during the positive half cycle. They tend to neutralize any positive ions created by a positive streamer from the rod, thus prohibiting the propagating of the streamer to the plane. At large spacings, the rod to plane values are higher than the plane to plane values.

They discussed about the dropping of dielectric strength in certain regions of pressure for fluorogases due to the property of electronegativity. It is possible to shift this region for practical purposes to a higher pressure range by mixing the gas with nitrogen. They have conducted the impulse strength of the fluorogases and nitrogen mixtures.

Works and Dakin<sup>6</sup> discussed in their paper about some of the

---

<sup>5</sup>G. Camilli, T. W. Liao, and R. E. Plump, "Dielectric Behaviour of Some Fluorogases and Their Mixtures", AIEE Transactions, vol. 74, 1955, pt. 1, pp. 634-642.

<sup>6</sup>C. N. Works and T. W. Dakin, "Dielectric Breakdown of SF<sub>6</sub> in Nonuniform Fields", AIEE Transactions, vol. 72, 1953, pt. 1, pp. 682-687.

anomalies in the dielectric breakdown of  $\text{SF}_6$  as functions of pressure and electrode separation in nonuniform fields. They worked with 1/16" diameter hemispherical to 6" diameter plane and point to plane. They explained that the conditions to produce a maximum in the spark-over voltage are a divergent field and a gas with electron attaching molecules. They discussed the effect of pressure on positive d-c breakdown. The negative d-c spark-over voltage beyond a critical pressure which depends upon field configuration is greater than that of positive d-c. They have also shown, after the maximum is reached, the rate of decrease of breakdown voltage with pressure is a function of field configuration. Breakdown KV of  $\text{SF}_6$  is six times that of  $\text{N}_2$ , which occurs in the region of maximum where corona precedes spark-over.

Berberich, Works, and Lindsay<sup>7</sup> investigated the breakdown behavior of the higher molecular weight perfluorocarbon vapors and mixtures of these with nitrogen. The term perfluoro indicates that all of the hydrogen in hydrocarbon has been replaced by fluorine. The electrodes, sphere to sphere, rod to rod (1/2"), and rod to plane were used. The results were compared with nitrogen,  $\text{SF}_6$ , and oil. Fluorine is the most electronegative of all elements and fluorine compounds are particularly effective in trapping electrons in the early stages of the gaseous breakdown process and, thereby, increasing the voltage at which final breakdown takes place. They have shown that the breakdown voltage

---

<sup>7</sup>L. J. Berberich, C. N. Works, and E. W. Lindsay, "Electric Breakdown of Perfluorocarbon Vapours and Their Mixtures with Nitrogen", AIEE Transactions, vol 74, 1955, pt. 1, pp. 660-666.



of perfluorocarbon vapors is extremely sensitive to electrode configuration. For rod to rod, as it is the severe case of divergent field, they found the positive impulse values are lower than the 60 cycle crest values, whereas, the reverse is true for the negative impulse values for mixtures with  $N_2$ .

The addition of 0.12 lb/cubic foot of  $C_7F_{14}$  to  $N_2$  increases the 60 cycle dielectric breakdown by a factor of about 3.5.

In the discussion, they have explained the increase in breakdown strength of gases containing electronegative molecules as the great affinity of electronegative atoms for electrons. Many free electrons are captured before they can reach ionizing velocities, thus streamer formation is inhibited. The slow negative ions formed through electron capture also reduce the positive space charge in the streamer, thus making a higher voltage before the streamer can cross the gap. They have shown also the breakdown strength increases with molecular weight or molecular size and the larger the molecule, the higher the breakdown strength.

They have finally concluded the breakdown strength of the perfluorocarbons is influenced not only by their molecular weight, but also by their chemical structure. They have recommended perfluorocarbons for electrical application due to their excellent properties; namely, flameproofness, thermal stability, and chemical inertness.

Pollock and Cooper<sup>8</sup> have investigated the effect of pressure on

---

<sup>8</sup>H. C. Pollock and F. S. Cooper, "The Effect of Pressure on the Positive Point to Plane Discharge in  $N_2$ ,  $O_2$ ,  $CO_2$ ,  $SO_2$ ,  $SF_6$ ,  $CCl_2F_2$ , A, He, and  $H_2$ ", Physical Review, vol. 56, 1939, pp. 170-175.



the positive point to plane discharge in  $N_2$ ,  $O_2$ ,  $CO_2$ ,  $SO_2$ ,  $SF_6$ ,  $CCl_2F_2$ , A, He, and  $H_2$  and of certain mixtures of these gases. They found with some gases, a complete refilling of the cell after a spark would raise the first subsequent measurement of corona initiation voltage and the corona initiation voltage can be lowered by x-ray irradiation.

They have observed at low pressure, with the positive point, there is a fairly wide corona region in all gases. It can be observed with an oscilloscope when the voltage is raised slightly above the onset voltage, the isolated pulses are replaced by another pattern which is termed as burst corona and named so by Loeb<sup>9</sup>. The burst pattern begins after one of the kicks which is produced by the intermittent corona is first observed.

In the region of intermittent corona for the positive point, they have compared it to a Geiger counter region. They have explained this as a single electron or ions approaching the point to produce an electron avalanche by collision of ionization in the high field region. The electrons produced flow to the point and the positive ions remain to distort the field and virtually to prolong the positive point. New avalanches produced by outside radiation will extend the space charge further into the gap. The streamer advances until it is extinguished in the low field region away from the point. They have explained that the sharp kicks just before breakdown indicate the formation of streamers from the edge of the burst region.

---

<sup>9</sup>Leonard B. Loeb, Fundamental Processes of Electrical Discharge in Gases, John Wiley & Sons, Inc.: New York, New York, 1939.

They have observed streamers from a positive point in  $H_2$ , He, A, and  $N_2$ , but they failed to observe a continuous burst corona pattern similar to that in gases which readily form negative ions.

They have explained the effect of pressure on spark curves by stating the Townsend's ionization coefficient. As  $\alpha/p$  varies approximately as  $E/p$ , where  $E$  is voltage gradient,  $\alpha$  then increases about as rapidly as pressure in the low pressure region. This linear increase in  $\alpha$  will then give rise to an exponential increase in negative ions.

They have discussed the effect of x-rays and diffusion also. At higher pressures, the x-ray irradiation lowers the gap strength. Diffusion has a role similar to negative ion formation in that it decreases the field at the tip of a streamer and in other regions where space charge gradients tend to be high. Diffusion may also increase spark voltages at which the maximum pressure appears.

Kip<sup>10</sup> discussed in his paper positive point to plane discharge in air at atmospheric pressure. He investigated the discharges on current voltage characteristic basis. All currents start abruptly, then increase linearly, and then more steeply with voltage until breakdown occurs. He has shown that the corona process in air is discontinuous involving alternate propagation and space charge quenching of positive streamers out from the point.

Attachment of electrons to form negative ions and then detachment of these electrons in the high field near the point provides a

---

<sup>10</sup> Arthur F. Kip, "Positive Point-to-Plane Discharge in Air at Atmospheric Pressure", Physical Review, vol. 54, 1938, pp. 138-146.

means of starting new streamers for self-maintaining corona process.

He has introduced a radioactive source in the gap region and has explained the sharp cut-off of corona current, as the voltage is decreased, due to lack of electrons for initiating new streamers. Initial current is found to increase, as the gap distance is decreased, and this is due to the change in field distribution and due to further extension of streamers into the gap.

Below a certain minimum gap distance, depending upon the point, he has observed the initial streamers travel completely across the gap and this highly efficient ionization at the cathode causes breakdown. He has observed also that above the initial current rise, the current increases as the square of the difference between the applied and offset voltage. The reciprocal of slope as initial rise in current is considered as effective resistance interposed by a weak field region of the gas.

In his paper, he has defined a new term which is "corona point distance". When the gap is less than a certain critical length, called the corona point distance, the corona process no longer occurs and the gap breaks down completely into a spark.

Trichel<sup>11</sup> investigated the mechanism of negative point to plane corona by studying the oscillographs. The corona starts when a field exists near the point sufficient for a positive ion to gain enough energy in its last free path to produce at least one electron. The value of

---

<sup>11</sup>G. W. Trichel, "The Mechanism of the Negative Point to Plane Corona Near Onset", Physical Review, vol. 54, 1938, pp. 1078-1084.

this energy depends upon the work function of the surface for secondary electron emission on positive ion bombardment. The oscillographs, obtained by him, indicate the negative corona current is composed of discrete pulses whose magnitude have a relationship to the corona current, point size, and gas pressure. The frequency of the current pulses appear to be independent of gap length. The frequency of oscillations are not affected by changes in the electrical constants in the discharge circuit outside the gap.

Fitzsimmons<sup>12</sup> studied the two facts: (1) The threshold field strength at which the various positive point corona phenomenon begin, including the effects of humidity and accumulation of oxide in the gap. He used confocal paraboloids. (2) He compared Meek's theory with the experiment.

He explained the results under the following subheadings, that is, in the order of phenomenon observed in positive point to plane corona: (1) Small intermittent and irregular preonset burst. Burst pulses begin to appear according to the oscillograph after the field at the point surface reaches a certain minimum value depending upon the size of the point and the air pressure. (2) Preonset streamers. He has found very little difference between the values for dry and moist air. According to Meek, the criterion for streamer formation at the positive electrode is that the radial field about the positive space charge in an electron avalanche attains a value equal to  $KX_A$  where  $X_A$

---

<sup>12</sup> R. E. Fitzsimmons, "Threshold Field Studies of Various Positive Corona Phenomenon", Physical Review, vol. 61, 1942, pp. 175-182.

is the field at the electrode surface and  $K$  is a constant between 0.1 and 1. The author found confocal paraboloids agreeing with Meek's equation and  $K = 0.1$ . (3) Steady burst corona. Air up to 55% relative humidity had little effect upon the onset fields for steady corona. With 65% relative humidity, the fields at the point for the different gaps do not agree with each other. This disagreement is explained as the extreme sensitiveness of the range of brush corona potential to slight humidity changes. (4) Spark breakdown. It is found that the effect of moist air is of no consequence, except for the very short gaps.

Kip<sup>13</sup> studied the positive point to plane corona in air at atmospheric pressure, especially on preonset region. He observed two types of current pulses by studying the oscillographs and photographs. At lowest voltages, he observed a glow around the point. At voltages near onset, streamers were observed which extend far out into the gap and which can propagate into a space charge gap. Streamer propagation and stable burst corona depend upon photoelectric ionization in the gas. Streamer length is found to depend primarily upon point size. For very fine needle points, it is hard to distinguish between burst and streamers.

By using a shielding screen to cut out the electrostatic pulse produced by streamers or bursts, it is possible to find the number of ions produced. This was found to be about  $5 \times 10^9$  ions per streamer and about  $2 \times 10^9$  ions per burst pulse. The time for positive ions to

---

<sup>13</sup> Arthur F. Kip, "Onset Studies of Positive Point-to-Plane Corona in Air at Atmospheric Pressure", Physical Review, vol. 55, 1939, pp. 549-556.

cross the gap was found to be about  $10^{-3}$  seconds and this will vary with the gap geometry.

Trichel<sup>14</sup> in his paper, regarding the mechanism of the positive point to plane corona in air at atmospheric pressure, discussed about the fluctuating character of the current. It was shown that in the self-sustained corona, the current is due to a large number of individual current pulses or bursts which are distributed over the surface of the point in regions of adequate field strength. The bursts are random in nature, regarding time, space, and intensity, and consists of many avalanches of electron ionization which flow into regions of high field strength caused by space charges. The electron avalanches are initiated in air by photoelectrons produced in the gas near the point. He has shown evidence of all these photographically to confirm the existence of bursts. The ionization produced is most intense at the point in the early stages and intensity of bursts increase with field strength.

In air, the self-sustaining corona requires a high enough potential to overcome the space charge and adequate current to supply photoelectrons and the formation of negative ions to insure that fluctuations shall not break off the discharge.

As the field at the point and clearing field increase, the bursts propagate further into the gap and ultimately form streamers from 6 to 11 mm long. Further, the streamers project towards the cathode and if

---

<sup>14</sup>G. W. Trichel, "The Mechanism of the Positive Point to Plane Corona in Air at Atmospheric Pressure", Physical Review, vol. 55, 1939, pp. 382-390.

these strike the cathode and create an active cathode spot, the return discharge produces a spark or an arc.

After reviewing several of these articles, the author has come to the following conclusions: Several engineers and physicists worked the same problem; namely, the discharge in gases.

The engineers worked with several gases and tried to find a gas which has very high dielectricity. Fluorine compounds are found to be the best dielectric, at any pressure.

The physicists concentrated on the mechanism of the breakdown with different electrodes and discussed it in terms of streamers and burst pulses in the gas. Most of them have worked on point to plane gaps and discussed it with the help of photographic pictures and oscillographs.



## CHAPTER III

### METHODS AND MATERIALS

Air and  $C_3F_8$ , which has the chemical name of octafluoropropane, were used in these experiments.

Electrode systems used in these experiments were  $3/4$ " diameter sphere to plane, point to  $1\ 3/4$ " diameter plane, point to point,  $1$ " diameter sphere to  $1$ " square plane, superimposed on a  $1\ 3/4$ " diameter plate,  $3/4$ " square plane to  $3/4$ " square plane, and  $1/2$ " square plane to  $1\ 3/4$ " diameter plane. Some of the investigators used the name rod for square plane.

The electrodes were cleaned by using sandpaper and fixed in the test cell. Screws of the test cell were tightened so that there would be no leakage. The initial micrometer reading was noted when the two electrodes touched each other. Gap settings were made by turning the micrometer screw which is on the top of the cell. Barometric pressure was noted. The test cell was evacuated by the evacuating pump and it was flushed with the gas, then evacuated again. The test cell was then filled with the gas which was maintained at the normal pressure by applying a positive pressure of  $760-p$ , where  $p$  is the atmospheric pressure, at that time. Air pressure was developed with the help of an ordinary cycle pump. The gas control equipment is shown in Figure I. Gas from the container was then passed through the  $H_2SO_4$  and  $NaOH$ .  $H_2SO_4$  and  $NaOH$  act as drying agents. If there are any dust particles in the gas, they will be trapped in these jars.



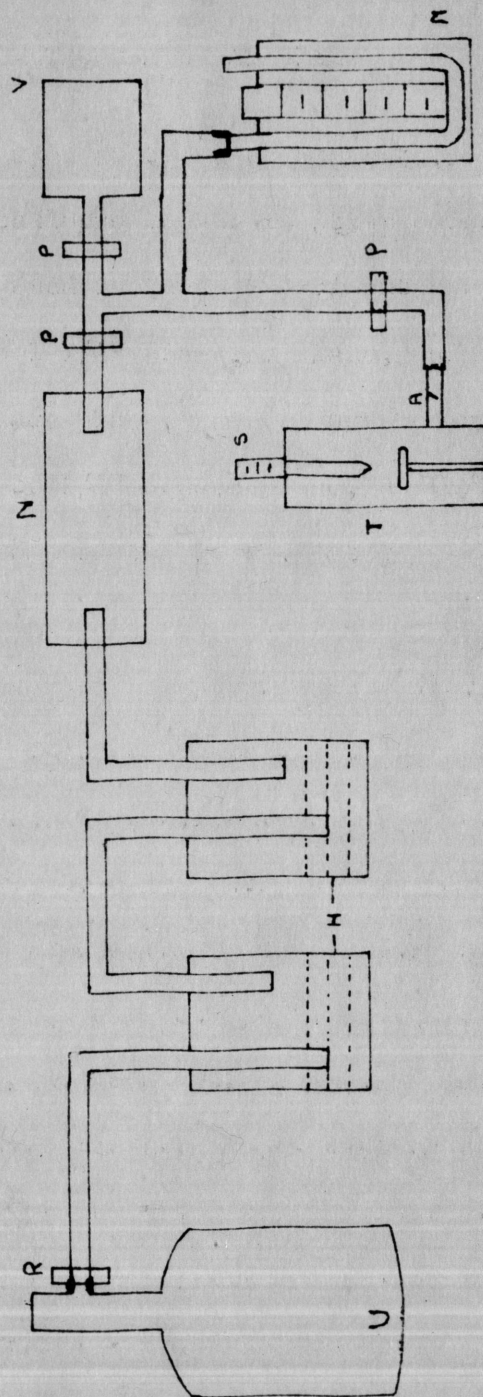


Figure I. Gas control equipment

A - Valve, H -  $H_2SO_4$  Jars, M - Manometer, N - NaOH Tube, P - Pinch cocks, R - Regulator,  
S - Micrometer screw, T - Test cell, U - Gas tank, and V - Vacuum pump.

The corona detecting circuit is placed in series with the test cell and ground. An oscilloscope connected to this circuit gives an uncalibrated indication of corona.

The test transformer is a 7.5 KVA, 75 KV voltage transformer supplied through a variac. The circuit breaker is equipped with three push button switches. The first is for closing the switch for the breaker; the second is to close the breaker for testing; and the third is for opening the breaker. Three indication lamps are located near the push button switches which are amber, red, and green in color. The amber indicates the closing of the breaker; the red indicates the test; and the green indicates off. The whole equipment is located in a copper screened room for safety. There is a door in between the test transformer and the control. This door is equipped with a switch so that the breaker could only be closed after closing the center door.

The main switch was closed first and then the oscilloscope was put into service. Sweep range of the oscilloscope was fixed at drive and gain at 0.01. In the beginning, it was tried with gains 1 and 0.1, but the bursts on the oscilloscope were indistinguishable from one system to the other electrode system, therefore, 0.01 gain was fixed for all the experiments.

The first push button was closed and then the test push button. The voltage was raised across the electrode gap by turning the wheel, which is located near the push button switches. The voltmeter on the breaker indicates the rms KV. It has two ranges, one is low from 0 to 30 KV and the other is high, 0 to 75 KV. In all the experiments, the

voltage is raised very slowly until breakdown occurs. At 90% of breakdown KV for 0.5 gap settings, pictures of the corona bursts on the oscilloscope were taken for some of the electrode systems using the two gases. For 1/2" square to 1 3/4" plane at every gap setting, pictures of corona bursts were taken at 90% of breakdown KV.

The type of film used for the camera was a 3000 speed poloroid land picture roll. Several time and aperture openings were tried. It was found that 1/50 of a second and 1.9 settings were the best for the corona bursts. These settings were used for all the pictures.

## CHAPTER IV

## BASIC THEORY

A. General Discussion

When voltage is applied between two electrodes and is raised to such a level that the electric field between the electrodes is high enough to ionize, a discharge occurs across the gap. If there are two electrodes of different sizes and they are separated, the field is concentrated at the electrodes. The fields with sharp points become sufficiently high enough for breakdown at these regions, long before a spark can propagate across the gap space. It can be expected that the breakdown can occur in two steps. First, breakdown at the electrodes, at one or at both, and ultimately a breakdown of the gap as a whole, that is, a spark.

A manifestation of this discharge at the electrodes is the emission of light sometimes accompanied by audible noise and by current fluctuations. The peculiar forms of these localized and partial breakdowns are named corona brush discharge and at lower pressures, glow discharges.

The spark defined by Loeb<sup>15</sup> as an unstable and discontinuous occurrence marking the transition from one, more or less, stable condition of current between electrodes in a gas to another one.

Often corona and spark breakdown are nearly simultaneous at low gap lengths; for example, in air for point to plane or point to point, the

---

<sup>15</sup>Loeb, op. cit.

bursts of corona will start just before breakdown. In order to understand clearly the phenomenon of breakdown, the mechanism and theory of spark were also dealt with.

The terms glow, brush, and corona characterize the different visual forms of the phenomenon.

At lower pressures, the luminosity is general and diffuse over the surface of the electrodes, which can be expected from the high diffusion of electrons at low pressure. This is called glow discharge.

At atmospheric pressure, the luminosity at the points is localized at the negative points of the small area, while at the positive points, it sometimes spreads as a thin film over the high field portions. This is termed corona proper.

Under other conditions, the luminosity extends out into the gap in the form of a brush of diverse geometry. This is called the brush discharge.

In breakdown, the electron is the initiating agent. When it is travelling in the gas under the field, it will produce some more electrons by collision with the gas molecules. If electrons were liberated continuously from a plate in a gas, the current flows in a linear fashion with respect to applied voltage. As the voltage is increased further, the current reaches its saturation value. When higher fields are applied, then the current will increase rapidly with potential, or in other words, the current increases exponentially in the form of a spark. At a certain field strength,  $F$ , suppose the electrons are producing  $\alpha$  new pair of ions/cm path due to collisions with the molecules of the



gas, the current can be expressed as

$$i = i_0 e^{\alpha x}$$

where

$i_0$  = initial current

$x$  = length of path

The quantity  $\alpha$  is a function of pressure,  $p$ , and the field strength,  $F$ . The value of  $\alpha$  depends upon the ability of the electron to ionize another gas molecule.

If  $E_0$  is the required energy to produce ionization, this will take place when the electron moves a mean free path distance  $\lambda_1$ , such that  $e \lambda_1 = E_0$  where  $e$  is charge on the electron. Mean free path distance is a function of pressure.

In this connection, a famous law discovered by Paschen in 1889 can be considered. The sparking voltage is a function of the product of pressure and distance. This law is followed from the extension of Townsend's theory. As the pressure is decreased, the breakdown voltage decreases almost linearly until the gas is quite rare and then voltage rises again. The minimum breakdown voltage occurs at critical pressure.

If spark breakdown is dependent upon concentration of ions inside or influenced by the presence or deficiency of ions in any region, then for the electrode arrangement in the gas, the law does not hold.

Townsend's theory, the foundation for the discharge in gases, will be discussed here very briefly. In his earlier study of the current between parallel plates with the applied voltage, the current first increases linearly to a certain extent and then the increase of current is less for a great voltage change. At a certain range, the current

increases very rapidly with little change in voltage. This increase of current was described by Townsend as the ionization of the gas by electron collision. Townsend introduced a coefficient,  $\alpha$ , to define the number of electrons produced in the path of a single electron traveling a distance of 1 cm in the direction of the field. The current flowing in the gap is given by  $i = i_0 e^{\alpha x}$  where  $x$  is the gap length.

In his measurements for parallel plate gaps, if the voltage is raised sufficiently, the current observed increases more rapidly than the equation explained before and, therefore, the secondary mechanism must be effecting the current.

The liberation of electrons in gas by collisions of positive ions with molecules and the liberation of electrons from the cathode by positive ion bombardment were both considered by him. The secondary emission from the cathode by positive ion bombardment is a major factor in low pressure discharges. Many investigators disagree with him regarding the liberation of electrons in the gas by this mechanism, as the positive ions cannot acquire sufficient energy and the particular field condition to ionize gas atoms on collision. These conditions were explained by streamer theory which will be explained later.

Townsend's equation is:

$$i = i_0 \frac{e^{(\alpha - \beta)x}}{\alpha - \beta} \quad (1)$$

Townsend's first coefficient,  $\alpha$ , is the number of new electrons created in the gas by an initial electron in its path of 1 cm along the field axis from the cathode. The second Townsend's coefficient,  $\beta$ ,

is the number of new electrons created by a single positive ion in advance of 1 cm along the field axis from the anode.

The  $i_0$  is the photoelectric current and  $x$  is the variable plate separation.

Two other equations developed with the help of Townsend's equations are:

$$i = i_0 \frac{e^{\alpha x}}{1 - \gamma (e^{\alpha x} - 1)} \quad (2)$$

$$i = i_0 \frac{\alpha e^{\alpha x}}{\alpha - \gamma \theta g [e^{(\alpha - \mu)x} - 1]} \quad (3)$$

Equations (1), (2), and (3) were taken from the literature cited<sup>16</sup>.

Equation (2) is one for the liberation of secondary electrons at the cathode by positive ion bombardment. The  $\gamma$  is the chance that a positive ion will liberate an electron from the cathode on impact.

Equation (3) is the equation for liberation of electrons by photoelectric action at the cathode. The  $\theta$  is the number of photons created per cm path of advance of an initial electron in the field direction whose frequency is such that they can liberate an electron from the cathode. The  $g$  is the geometrical factor of value 0.5 (approximately) which depends upon the fraction of photons in the gap reaching the cathodes. The  $\gamma$  is the fraction of the photons reaching the cathode that succeed in actually liberating electrons from the cathode. The  $\mu$  is an absorption coefficient of the photons in the gas.

---

<sup>16</sup> Leonard B. Loeb and John M. Meek, The Mechanism of the Electric Spark, Stanford University Press: California, 1941.



Townsend's classical theory of mechanism of spark discharge is on the basis of measurements made at high values of  $x/p$ , the ratio of field strength to pressure and at low values of  $p\delta$ , the products of pressure times gap length. His theory also explains the mechanism of sparking under ordinary conditions for longer gap lengths at atmospheric pressure and above.

Many investigators have indicated that for values of  $p\delta$ , near and somewhat above the minimum sparking potential, the theory is relatively accurate. In the early forties, it was found that the theory was entirely of no use when applied to sparks for  $p\delta$  greater than 200 mm of mercury. The reasons for this conclusion can be explained as follows:

1. The time required for the breakdown mechanism to materialize, was found by several investigators to be of the order of  $10^{-7}$ , or even less, for 1 cm gap. These time intervals are far below the micro-seconds required by the positive ion movement.
2. At atmospheric pressure, the sparking potential has been found to be independent of the cathode material to a very high degree. The theory above even is insensitive to the value of  $\gamma$ , at higher pressures, having a definite dependence of the order of 10% of the value of  $\gamma$ .
3. In longer spark gaps and in positive point corona, at atmospheric pressure, the discharge is not dependent upon the cathode character.
4. The appearance of sparks in measurement of Townsend's coefficient,  $\alpha$ , at higher pressure and sufficient value of gap distance with no measurable value of  $\gamma$ , is no longer applicable at higher values of pressure and gap lengths.
5. Visual observation of sparks indicates that the sparks follow in narrow channels and this is incomparable with the conduction of currents in a gas caused by accumulations and movements of positive ion.
6. In Townsend's theory, only one electron is required to initiate the spark and the greater the number of photons, incident

on the cathode by external means, the more rapidly the space charge accumulations occur. The formative time lags should, on that theory, decrease as the illumination intensity of the cathode increases. This is true for low values of  $p\delta$ . For high  $p\delta$ , there is no change in formative time lag.

Due to all these objections to the classical theory of Townsend, several investigators tried to find a new mechanism, which did not conflict with the experimental results. Finally, this mechanism was found, based on streamer theory.

The streamer theory is discussed by Meek<sup>17</sup> in his theory of spark discharge. A brief discussion of the same will be given here. The breakdown of a uniform field is considered to occur by the transition of an electron avalanche proceeding from cathode to anode into a self-propagating streamer, which develops from anode to cathode to form a conducting filament between the electrodes.

A streamer will develop when the radial field about the positive space charge in an electron avalanche attains a value of the order of the external applied field. The photoelectrons produced in the gas, in the immediate vicinity of the avalanche, will not only be accelerated in the direction of the external applied field, but will also be drawn into the stem of the avalanche. It has been shown by several people like Loeb, Kip, and Cravath, etc., this streamer propagation depends upon photoionization in the gas. In this way, the positive ion space charge attracts photoelectrons from the surrounding space in large numbers to start a self-propagating streamer. For lower values of

---

<sup>17</sup>J. M. Meek, "A Theory of Spark Discharge", Physical Review, vol. 57, 1940, pp. 722-728.

applied field, where the multiplication of ions in the avalanche is insufficient to produce a radial field of the same order of magnitude, as the external field, photoelectrons produced in the gas proceed to the anode and are not deflected to the main avalanche.

One can summarize the experimental results of his experiments with this theory as follows:

1. The mechanism depends upon photoionization which can be observed.
2. It is necessary that the density of the positive ion space charge, created in an electron avalanche, is sufficient to draw in photoelectrons. Ionization by collision makes the positive space charge into conducting plasma for further development of the streamer.
3. Independence of cathode material for long sparks is in confirmation with the observation.
4. It agrees with time lag studies. When a potential is applied to a gap in excess of the minimum to cause breakdown, mid-gap streamers will develop and the time lag is reduced. For this case, an electron avalanche, which originates at the cathode, will develop the required density of positive ions to cause the initiation of a streamer before the anode is reached. The reduced distance, which the avalanche has to travel before it produces a streamer, makes it probable that several streamers can start.
5. At the sparking threshold, the chance of spark depends upon (a) the chance of a single electron avalanche, which produces at the anode or in the mid-gap region, and (b) the success of the space charge can photoionize the gas molecules.
6. It agrees with the tests in a cloud chamber.
7. It can be shown that the field distortion produced by cumulative ionization with high densities of photoelectric current gives a lowering of sparking potential, as can be expected.
8. It explains the filamentary character of spark breakdown and, at high pressures, the zig-zag character and the branching.

9. It explains that at lower  $x/p$  and higher  $p \delta$ , sparking occurs before the values of the second coefficient,  $\nu$ , can be observed.
10. A slight deviation of this theory is consistent with the experiment.
11. The theory is extended to the explanation of sparks of all lengths at higher  $p \delta$  in air.
12. This theory can be applied to the breakdown of unsymmetrical gaps, where the field distribution is known. It can be applied to either surge pulses or static breakdown.
13. Finally, the self-propagating modified for longer sparks coincide with pilot streamers in Schonland mechanism.

This theory is successful and agrees with the results of several investigators.

#### B. Field Mapping

The field mapping gives the physical concept of the field which can be obtained in no other way. This way of analyzing electrical stresses of electrode configuration will be very useful.

Here the field analysis serves two useful purposes: (1) It can determine the magnitude of the electrical stresses in the critical areas and at what voltage level, there is likely to be corona; and (2) it gives the information as to the best electrode arrangement so that maximum benefit can be derived from the shielding influence of adjacent electrodes.

With the field mapping, several problems can be solved. They are: (1) Determination of surface charge distribution on irregular shaped conductors and on any electrode systems; (2) determination of magnetic flux density distribution in irregular air gaps; (3) calculation

of capacitance between irregular shaped conductors; and (4) calculation of reluctance of relatively long air gaps with fringing considered.

### General principles of field mapping, line, and tubes of force

If a charged body is placed near the region of another body, the charged bodies will be acted upon by a force. This force has a magnitude and a direction depending upon the charge and the particular point at which the small charge is placed. If this charge is so small that it can have little influence on the highly charged body, then it could be said that, the force is a measure of the strain in the medium produced by the charge. One can draw a vector with the magnitude and the direction of force. This vector is called a line of force.

Since there are an infinite number of points on the charged body (for instance on an electrode), an infinite number of lines of force can be drawn. It is necessary to ascribe a finite amount of force, which the line exerts and an area to the line, that is, the line becomes a tube. For this work, these tubes are assumed to be approximately rectangular in area. The number of tubes, which is finite, is a measure of the amount of charge on the electrode.

### Equipotential surfaces

The above mentioned tubes extend from a region of high potential to low, and it can be assumed that the potential falls off gradually from the higher to the lower. With a suitable measuring device, the potential contour lines can be found. The points, which are all at the same potential, form a contour line or an equipotential line. These

will lie on a surface, enclosing one of the electrodes. The equipotential surface would be perpendicular to the tubes of flux, at all points.

For example, for the two oppositely charged round end rods, projected towards each other, the flux extends across from one to the other, filling completely the whole space. An equipotential surface would look like paraboloids of revolution about the axis of the rods.

In flux fields, there are three types: (1) One dimensional; (2) two dimensional; and (3) three dimensional.

In the field between large parallel plates, the flux will flow straight. If one takes a square element of area on one plate and moves it across the other in such a manner as to enclose all the flux, which is terminated on the area, then one will cut out a right parallelepiped with a square base. This tube does not vary in width or depth. Such a field is called one dimensional.

Suppose the upper plate in the above example were folded, then the flux tube would be curved. If one took a square base and carried it as before so as to find the flux tubes, one would find that the depth of the tube did not change, but width did change, or width increased towards base. For all the tubes, the variation may be in width and length only, so this field is called two dimensional.

Suppose the upper plate is curved about a centerline, then if a square base is taken and followed out the flux tube, one would find the increase in width and depth towards the base. All the dimensions can vary in this case, so this is called a three dimensional field.



### Procedure in mapping

In plotting these fields, it is generally assumed the iron or any other metal of the electrode system has infinite permeability as compared to air. The flux lines will leave the top electrode and enter the bottom electrode, which is at the earth potential, at right angles. Flux flows from the high voltage region to the low in a path so that the total resistance or flow is a minimum.

### Laws to be observed for the flow of flux

1. The direction of flow is always normal to the direction of equipotential lines.
2. The quantity of flux flowing through a given element of volume varies directly with potential difference between opposite faces and inversely as the elastance.
3. In passing from one medium to the other, the flux tubes are refracted so that the ratio of the tangents of the angles made with the normal are directly proportional to the dielectric constants of the two media.

These laws are from unpublished material by M. L. Manning and others.

### Solution of one, two, and three dimensional fields

In each case, the flux tubes could be cut into several sections, by drawing equipotential surfaces. This is flat for a one dimensional field, singly curved for a two dimensional field, and doubly curved for a three dimensional field.

In a one dimensional field, there would be any two parallel planes perpendicular to the plates for the flux tube. In two dimensional, the planes would be in addition, perpendicular to the edge

described before. In the three dimensional field, one would use planes perpendicular to the plates and placed so as to pass through the center line, thus cutting out a wedge shaped section.

For the solution of one and two dimensional fields, the electrode boundaries will be given, then it is necessary to insert the flux and equipotential lines. In drawing the flux and equipotential lines, there is considerable estimation. Experience counts much. In several cases, it would be better if there were equal amounts of flux flowing through the tubes, then the tubes have to have equal elastances by law No. 2. Elastance is proportional to the ratio of length/area. Since for one and two dimensional fields, area is directly proportional to the width of the tube. The depth of the tube is constant and equal to unity. For convenience, the ratio of length to width is taken as unity (curvilinear square).

Moore<sup>18</sup> in his paper about mapping techniques applied to fluid mapper patterns discussed about the curvilinear squares. To map a tube, one has to start at one end and fill in with full curvilinear squares until a part of a square or remainder is left at the other end. When three boundaries are given, to locate the fourth, he suggested a method called the "circle in method". To circle in a square, select a circle of the most suitable size in the Lietz tool, then place the circle touching the three edges and draw a circle tangent to the three boundaries. The fourth side will be the tangent to the circle. This method

---

<sup>18</sup> A. D. Moore, "Mapping Techniques Applied to Fluid Mapper Patterns", AIEE Transactions, vol. 71, 1952.



is very useful in the evaluation of a tube, in terms of relative ohms. With this map, one can locate the desired equipotential lines.

For a solution of a three dimensional field, the field section is wedge shaped. In this case, one has to take depth into consideration. Here the elastance is proportional to  $\text{length}/(\text{width} \times \text{thickness})$ , therefore, if thickness changes, length/width must be changed, so as to keep the elastance constant. Suppose an element of two inches from the center line has equal length and width, and one has to draw another element about four inches from the center line, having the same elastance as the first one, then the length must be twice the width, since in the second case, the depth is doubled. One can assign arbitrary values for length/width by using the above rule. One can then draw the flux lines and equipotential lines as before into curvilinear rectangles, instead of squares. If these rectangles do not fall at a point, theoretically, one has to subdivide the map into infinitely small rectangles before testing for the correct shape. Before starting the map, one can fix the ratio lines parallel to the axis and assign arbitrary values for the length/width.

In choosing the 1:1 line, one has to consider two points: (1) As it is more easy to draw accurate squares than rectangles, one has to see that this line falls in the important region; and (2) it must not be placed very close to one side of the field as the rectangles will become flattened and it is hard to work with them.

In his discussion, the field maps of the electrode systems will be given here for a gap distance of 0.5".

In all the maps drawn, a few large elements were drawn first and divided into smaller and smaller subdivisions, whenever it was necessary. It was observed, if the field is subdivided by any three equipotential lines and correspondingly flux lines, it is easy to visualize the inaccuracies of the field, when shifting the lines here and there to see if the map is improved or not. If one has taken seven or more equipotential lines, it is enormously difficult to change the lines, as one cannot improve one region at the expense of another. Therefore, shifting of a line should be made only when it is clear that it will make all angles and areas correct, corresponding to that region.

In drawing these maps, large areas were taken into consideration first, then the 50% equipotential line was drawn. The flux lines were then inserted to give the shapes of areas desired and these were checked and rechecked until all the lines, angles, and areas were in approximately correct positions, so that visually the errors could not be detected. The next set of subdivisional lines were then inserted and the errors were corrected until they were below the limit of visual check. In all these maps, the angles should be accurate. Moore pointed out that, whatever the shapes of the areas, some possible condition could be imagined, but a skewed angle represents nothing at all.

In these maps, all the electrode systems have cylindrical symmetry, therefore, only  $1/4$  of the field is shown here. Except for the square plane to square plane electrode system, all the other fields of the other systems are three dimensional. All the maps drawn here are approximate. In drawing all these, consideration has been taken that,

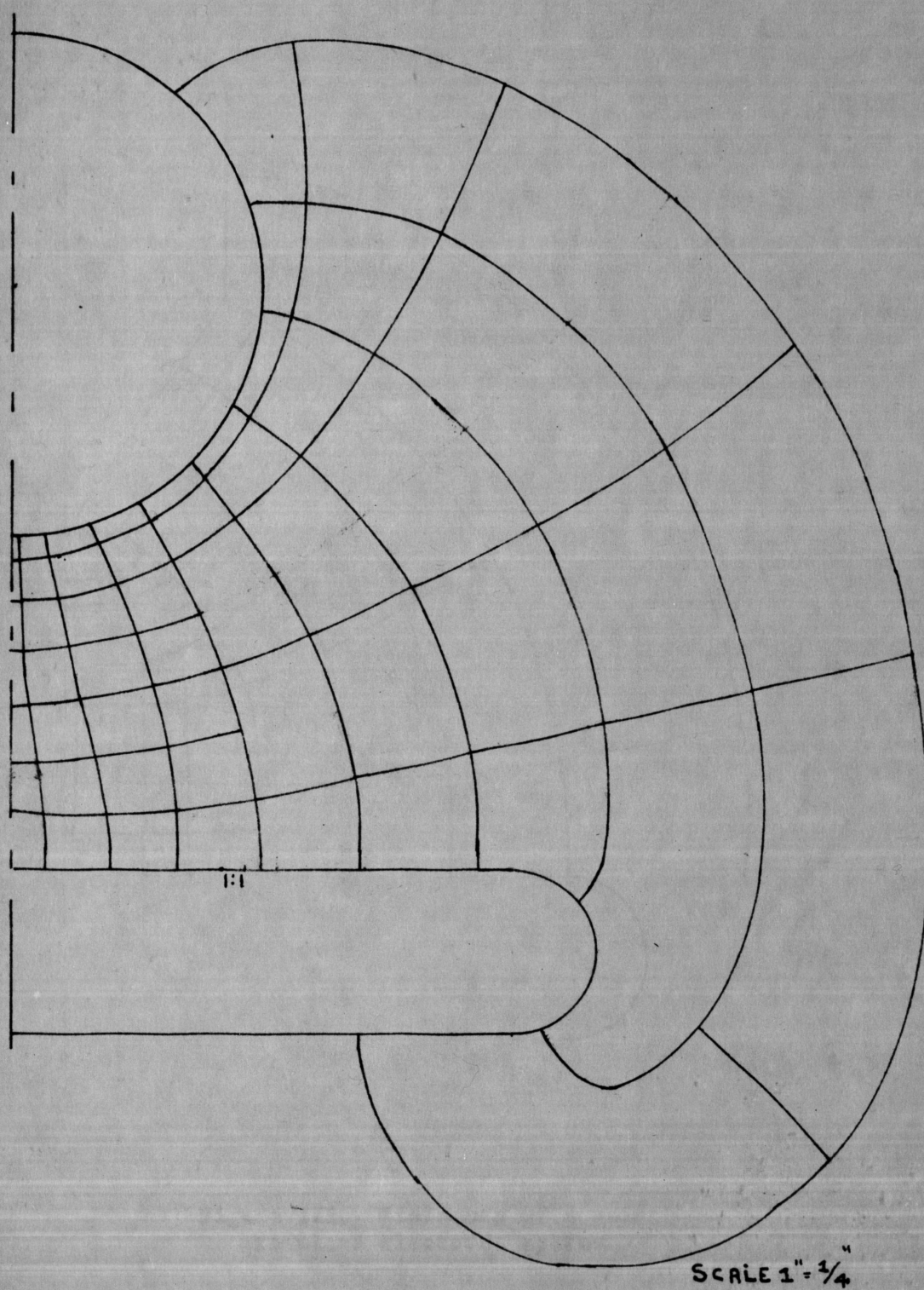
the bottom electrode is at earth potential. The gap distance is 0.5". All the flux lines leave or reach the electrodes at right angles.

Figure II is a three dimensional field of  $3/4$ " diameter sphere to  $1\ 3/4$ " diameter plane, the edges of the plane being rounded. First, the ratio lines were fixed and then the 50% equipotential line was drawn. The flux lines were inserted and the tubes were adjusted into squares in the 1:1 region. The angles and rectangles, in the other region, were also adjusted as the map is a three dimensional field.

Figure III is a three dimensional field map of a sharp point to  $1\ 3/4$ " diameter plane. The map is constructed as before. One can observe the field around the point is highly stressed.

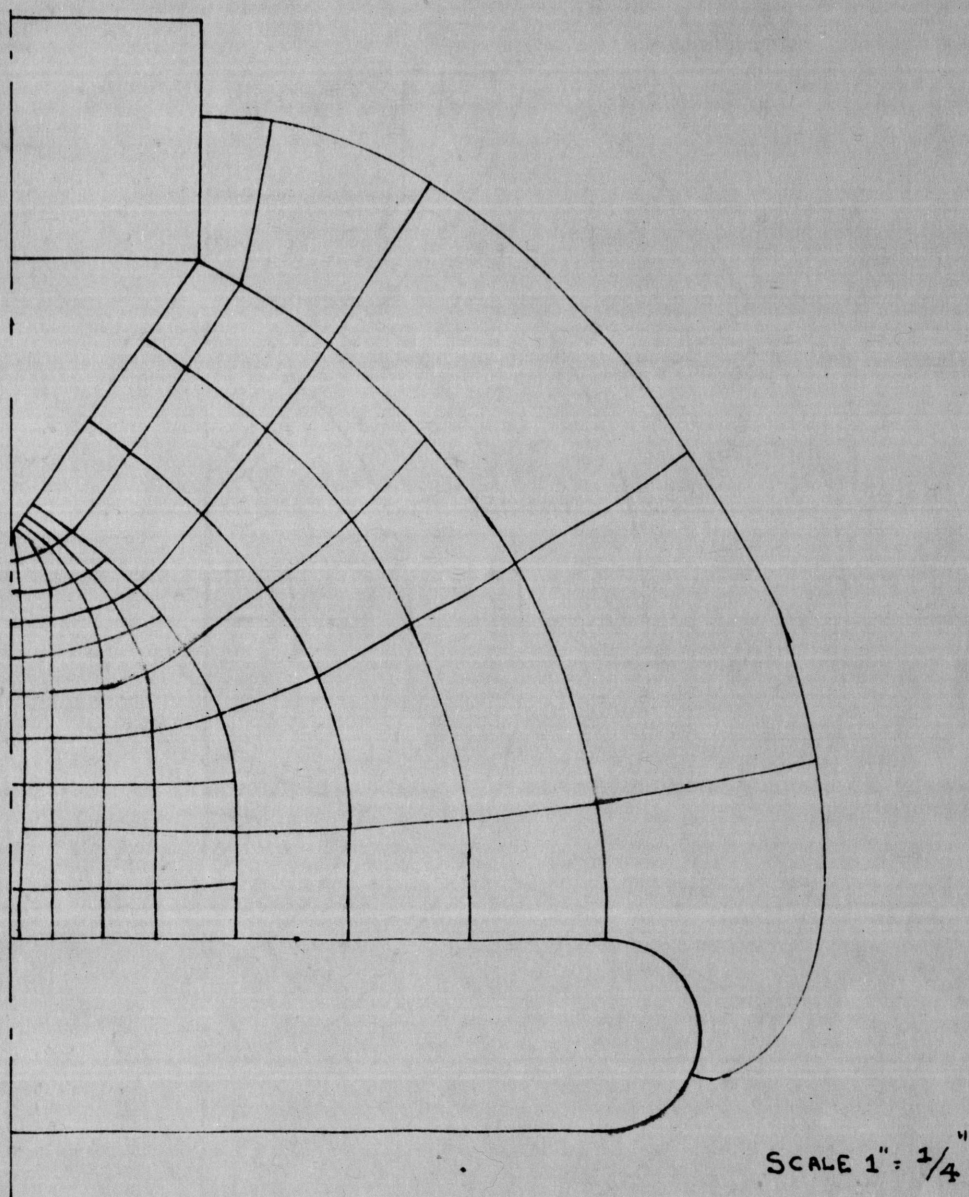
Figure IV is a three dimensional field map of point to point. One can observe that, the stress varies from the top to the bottom electrode, even though the two electrodes are of the same dimension. The field near the top point is highly stressed. For these two maps, the field near the point is stressed highly, since the points are sharp points.

Figure V is a three dimensional field map of 1" diameter sphere to 1" square plane, superimposed on a  $1\ 3/4$ " diameter plate. Here, one has to use the property of superposition. First, the square plate was taken into consideration and the field was sketched. The circular plate was then taken into consideration and the map was constructed with the sphere to circular plane. The map of sphere to square plane was superimposed on the second field. The squares and rectangles were then checked and the correction process applied as described before.



**Figure II. Field map of a sphere  
to plane electrode system**





**Figure III. Field map of a point  
to plane electrode system**

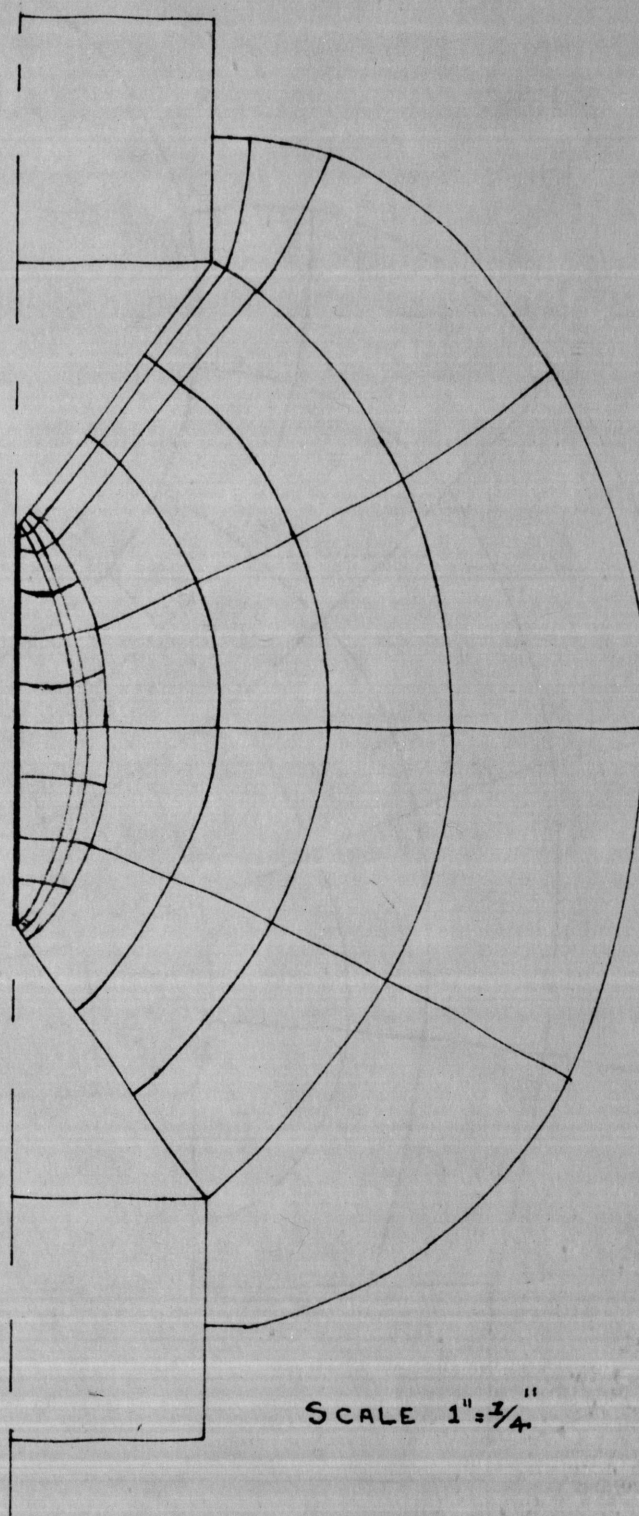


**Figure IV. Field map of a point  
to point electrode system**



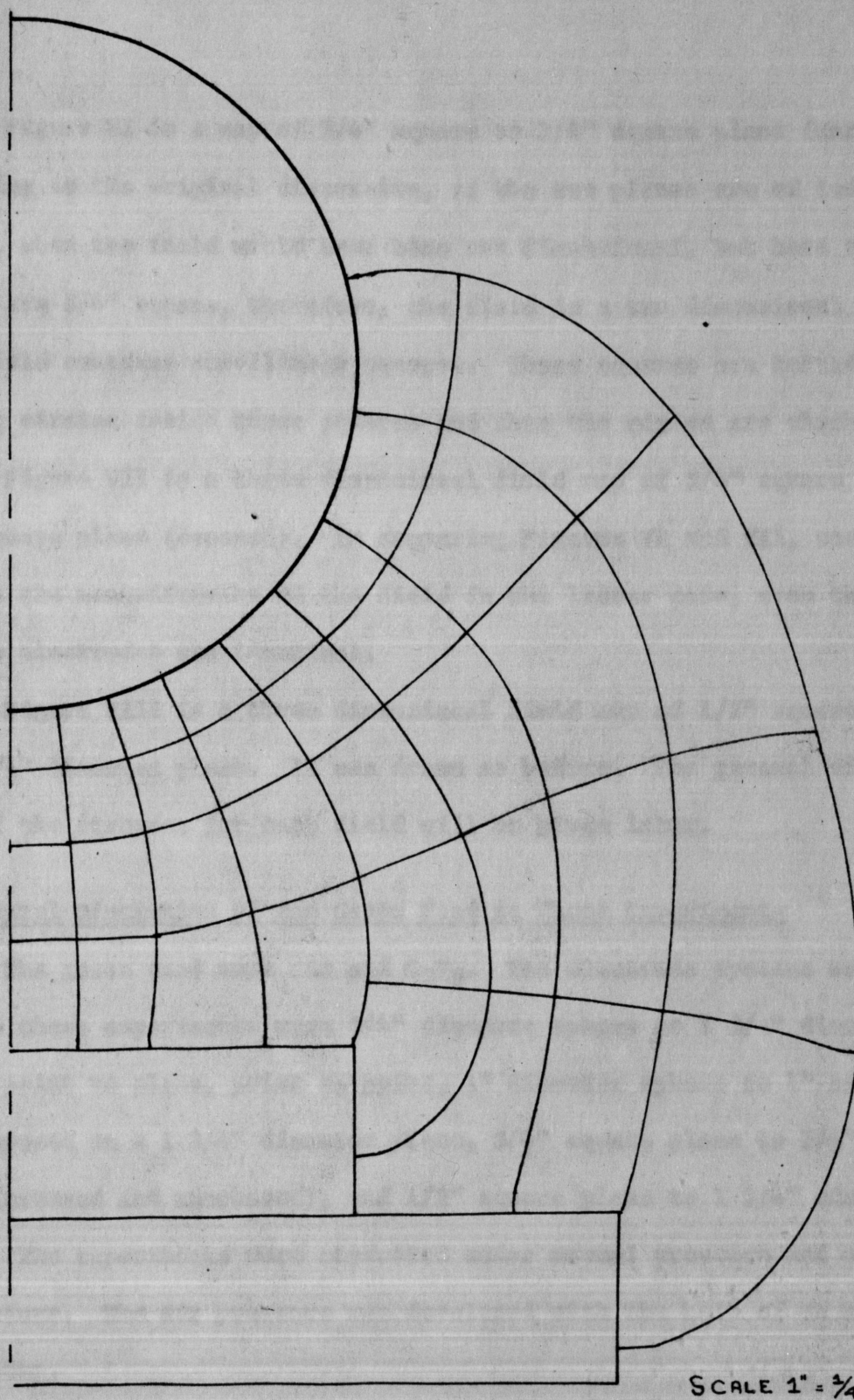


Figure V. Field map of a sphere to square plane, superimposed on a circular plane electrode system

Figure VI is a map of  $3/4$ " square to  $3/4$ " square plane (uncrossed). According to the original discussion, if the two planes are of indefinite length, then the field would have been one dimensional, but here the plates are  $3/4$ " square, therefore, the field is a two dimensional one. This field contains curvilinear squares. These squares are tested by drawing circles inside these squares and then the angles are checked.

Figure VII is a three dimensional field map of  $3/4$ " square to  $3/4$ " square plane (crossed). In comparing Figures VI and VII, one can observe the nonuniformity of the field in the latter case, even though the two electrodes are identical.

Figure VIII is a three dimensional field map of  $1/2$ " square plane to  $1\ 3/4$ " diameter plane. It was drawn as before. The general discussion of the stresses for each field will be given later.

### C. General Discussion of the Gases Used in These Experiments

The gases used were air and  $C_2F_8$ . The electrode systems used to perform these experiments were  $3/4$ " diameter sphere to  $1\ 3/4$ " diameter plane, point to plane, point to point,  $1$ " diameter sphere to  $1$ " square, superimposed on a  $1\ 3/4$ " diameter plate,  $3/4$ " square plane to  $3/4$ " square plane (crossed and uncrossed), and  $1/2$ " square plane to  $1\ 3/4$ " diameter plane. The experiments were conducted under normal pressure and at room temperature. The air pressure was developed with the help of an ordinary cycle pump.

The streamer theory will be used to explain the breakdown phenomenon. The discharge of gases depends mostly upon the photoionization in the gas. The process of photoionization occurs most efficiently



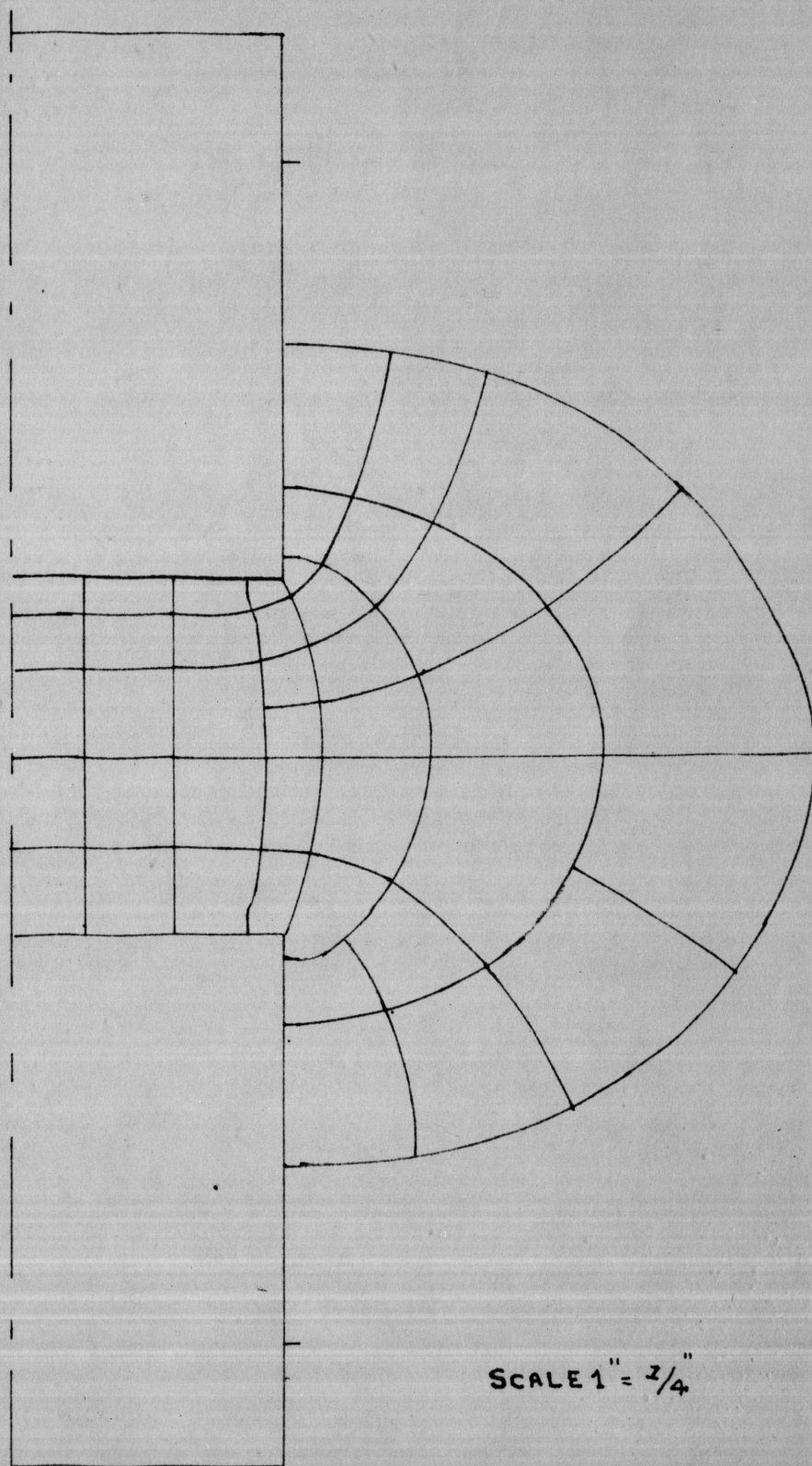


**Figure VI. Field map of a square plane to square plane (uncrossed) electrode system**

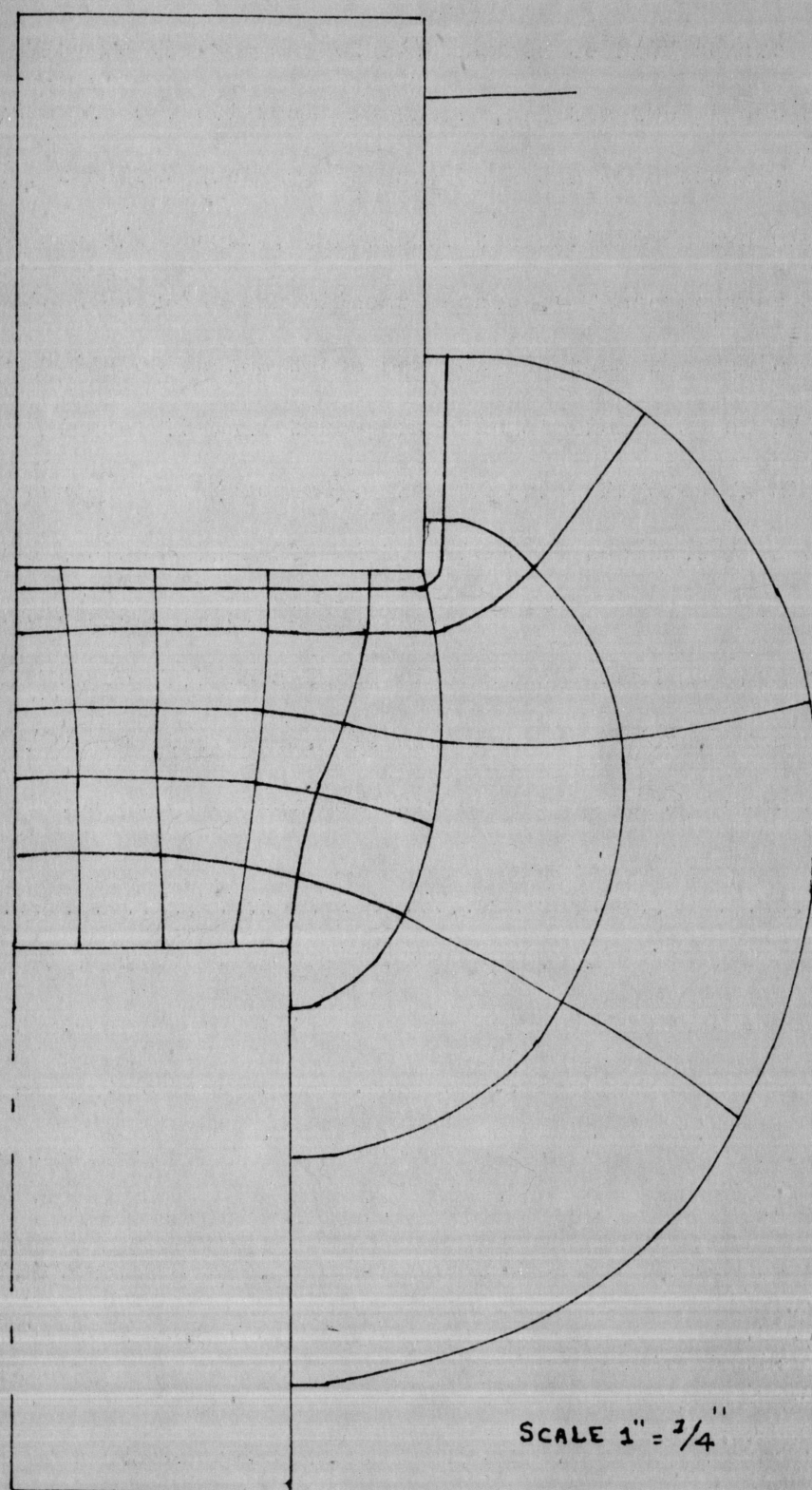
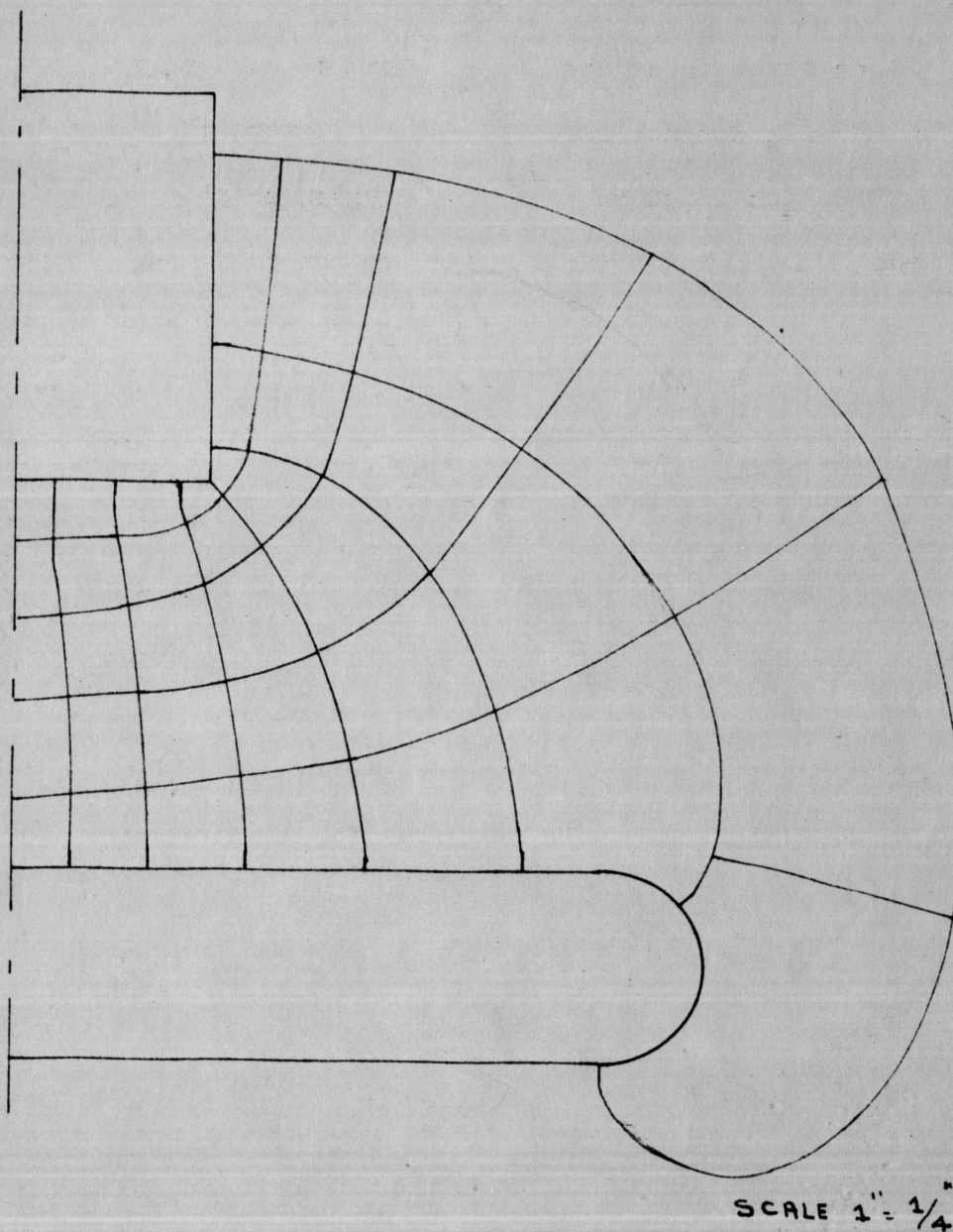


Figure VII. Field map of a square plane to square plane (crossed) electrode system





**Figure VIII. Field map of a square plane  
to circular plane electrode system**

in mixed gases or in gases where metastable states are abundantly produced. This is due to the fact that in a mixed gas, one constituent has an ionization potential which is lower than the higher state of excitation of another constituent.

When compared to  $C_3F_8$ , air has less breakdown voltage. It is almost half at the gap spacing of 0.5" for the square plane to 1 3/4" diameter plane, due to air being a combination of several gases,  $N_2$ ,  $O_2$ , rare gases, etc. The reason for the low breakdown voltage is that air is a mixture. In air, the efficiency of photoionization is such that the discharge mechanism operates through electrons generated by photoionization in preference to the liberation of electrons by positive ion bombardment.

The gas,  $C_3F_8$ , even though it is a compound of carbon and fluorine, can be considered as a plain gas like  $N_2$ , since this does not have the properties of a mixture. The unusually high dielectric strength observed in  $C_3F_8$  is caused by the electronegative character of the fluorine. Electronegativity is the attraction of an atom for the electrons which bind it in a stable molecule, or simply is the ability to consume free electrons. Any gas which does not form negative ions is unlikely to have high dielectric strength.

Fluorine is the most electronegative of all elements. Fluorine containing compounds can be expected to have higher dielectric strength than most other electronegative gases. Another reason given by Berberich for higher dielectric strength of these is that fluorine containing compounds is particularly effective in trapping electrons in

the early stages of the gaseous breakdown process, thereby increasing the voltage at which final breakdown takes place. This is one of the properties of electronegativity.

It was explained that the discharge of gas depends upon the efficiency of photoionization. The efficiency of photoionization can be defined as the number of excited atoms or ions formed by an electron in 1 cm thickness of gas at 1 mm mercury and at 1°C. The probability of excitation or ionization at a collision is found by dividing the efficiencies by the number of collisions made.

Considering stability of the ions, the stability of negative ions is measured by the electron affinity to the neutral particle. This is also the energy to detach an electron from the ion. The higher the electron affinity, the greater the stability of the ion. The  $O_2$ ,  $F_2$ , and  $Cl_2$  have higher electron affinity than any other gas. For the gases that are being considered,  $C_3F_8$  contains a larger percentage of fluorine than air contains in percentage of oxygen. The average number of collisions which an electron must make before attaching itself to a neutral gas molecule is  $\delta$ . Noble gases,  $N_2$  and  $H_2$ , have the value of infinity, but air has only  $2 \times 10^5$ . These values can be considered as the probabilities of attachment.

Negative ions play an important role in the discharges. It is complicated, due to the attachment and detachment process. Electron affinity can be described as a process,  $M + e \rightarrow M^{-1}$ , where  $M$  = neutral ion,  $M^{-1}$  = negative ion, and  $e$  = electron. This process indicates the energy change when an atom or molecule forms a negative ion by electron

attachment. The halogen atoms have the highest values, followed by oxygen, carbon, and sulphur, in diminishing order. Nitrogen and helium have negative values, which indicate that their negative ions are extremely unstable or nonexistent. In the gases used, air has a large percentage of nitrogen, therefore, the negative ions in air are unstable and have less breakdown voltage. Fluorine has the highest electron affinity, 4.1 ev and nitrogen has -0.6 ev; that is why  $C_2F_6$  has higher dielectric strength.

The ionization potential, another property of a gas, can be considered sometimes the dielectric strength of the gas. It can be represented as  $M \rightarrow M^+ + e$ . A positive ion and an electron are obtained from a neutral atom or molecule.

As a highly energized electron is assumed to be the initiator of the discharge process, it can be assumed that electron avalanches can start in this way, if enough molecules become involved in the action. If all matter produces positive ions and electrons, the potential of ionization varies for each substance. The values are  $F_2$  - 18.6 ev,  $N_2$  - 14.5 ev, He - 24.5 ev, and C - 11.2 ev. Inspection of these values show that helium, the weakest dielectric gas, has the highest ionization potential, so this property of a gas does not give a true evaluation of the dielectric strength.

Electron trapping is closely associated with electron affinity. The conditions controlling electron trapping or attachment are: (1) Pressure of the gas; (2) velocity of the colliding electrons; (3) molecular cross section of the particular gas molecule; (4) electron affinity; and (5) temperature.



Only slow electrons, that is with energies under 5 ev, will attach the molecules. Fluorine containing compounds are effective in trapping electrons in early stages of breakdown, thus raising the breakdown strength.

Deposits of carbon were observed when using  $C_3F_8$  on the electrode systems after the spark occurred.

One can conclude that no single factor can be entirely responsible for dielectric strength, but the combination of physical and electrical properties in a substance produce the resultant strength or weakness.

Finally, with all the above explanations, one can justify that  $C_3F_8$  has high dielectric strength and air has less. The only disadvantage of  $C_3F_8$  is the deposits of carbon during spark-over.

#### D. Breakdown of Gases Considering the Electrode Configuration

As explained in Chapter II, tests were conducted under normal pressure and at room temperature. Breakdown voltage versus gap distance for the various types of electrodes were plotted in Figures IX to XVII.

Corona breakdown depends upon several factors. Gas is the primary factor which was already discussed. The other factors are: (1) Application of voltage with respect to time; (2) pressure; (3) temperature; (4) electrode systems; (5) gap distance; (6) roughness of the electrode; and (7) volume occupied by the gas between the electrodes.

In these experiments, voltage is applied very slowly so this factor will not be in the discussion. Pressure is also maintained constant at normal pressure so this factor also will not be in the data. The temperature does not effect the value of breakdown voltage, unless

the temperature is raised abnormally high. Here the temperature is the same as room temperature, which was nearly constant. Gap distances of 0.1", 0.2", 0.3", 0.4", and 0.5" were used in the experiments.

At low pressures and at atmospheric pressures, the electrode plays an important role in the breakdown. The chemical nature of the electrodes will not have much effect, but the shape of electrodes has large effect particularly, if the electrode system contains points or corners. Cleanliness of the electrodes also effect the breakdown value. They should be free from films of oil, grease, organic material, finger prints, films of oxide, etc. Before fixing the electrodes, they have to be polished with an abrasive.

The electrodes should be smooth. Rough points or pits left by previous discharges, where heavy currents follow, lead to alteration in breakdown potentials, due to brush discharge, as do bits of oxide of microscopic size.

Point to point electrode system has the least volume occupied by the gas. This can be observed in the breakdown KV, as it has the lowest breakdown KV of all the other electrode systems. This effect will be predominant in effecting the breakdown KV, when the gap spacing is low.



## CHAPTER V

## RESULTS AND DISCUSSION

A. Systems Used in Tests

Breakdown strength of each pair of electrode systems will be discussed separately with the help of curves of breakdown KV versus gap length, flux plots, and pictures of oscilloscope pattern of corona bursts.

Corona bursts were observed for the two gases with the various electrode systems. At 90% of breakdown KV of the concerned system, the oscillographic pattern of the corona bursts were studied with the help of a camera. The settings used on the camera were 1/50 of a second and 1.9 spot. The gain of the oscilloscope was fixed at 0.01.

3/4" diameter sphere to 1 3/4" diameter plane

The breakdown curves for this system are shown in Figure IX, the field plot in Figure II, and corona bursts in Figure XVIII. Breakdown KV of  $C_3F_8$  at small gap distances is little more than twice that of air at the corresponding gap distances. As the gap distance increases, the slope of the curve for  $C_3F_8$  is more than that of air. At 0.5" gap distance, the curve for air became flattened. Breakdown KV of  $C_3F_8$  is more than twice that of air at 0.5" gap distance. As one can observe from the flux plot of this electrode system, the field is uniform. The breakdown KV is the highest of all other electrode systems at small gap distances for both the gases. The breakdown KV will be actually less than the pointed electrode system for both the gases at very large gap

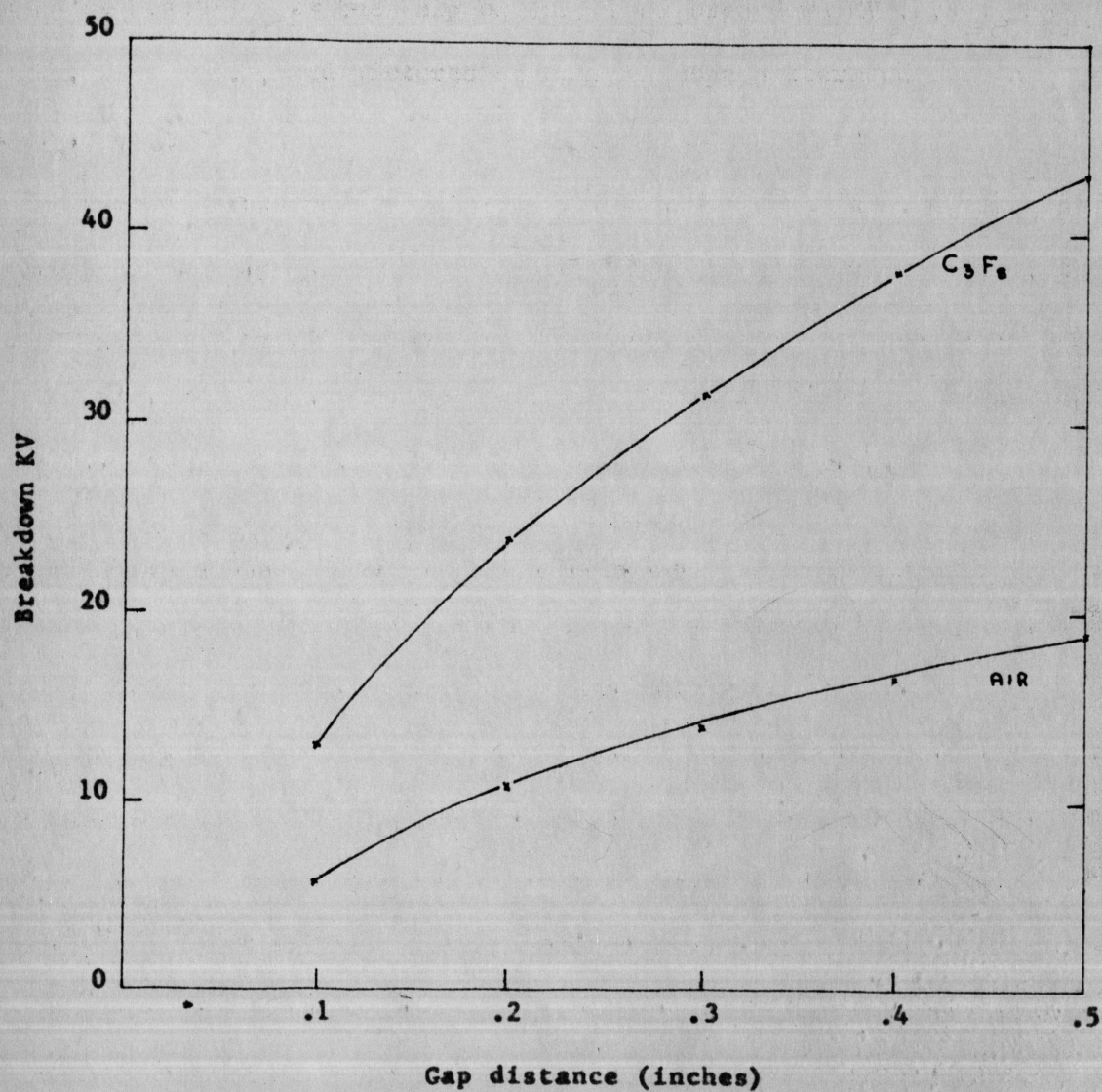


Figure IX. Breakdown strengths of  $C_3F_8$  and air with the sphere to plane electrode system

distances.

In cases of  $C_3F_8$ , at 85% of the breakdown KV, corona bursts started. At 90%, the bursts were very low as one can see from Figure XVIII-A. For air, bursts were considerably more as can be seen in Figure XVIII-B. This is due to the formation of negative ions, in the case of electronegative gases, so the streamers and the bursts will be less.

In this electrode system, the edge of the 1 3/4" diameter plate is smoothly curved. A rough edged electrode of the same size was tried. Breakdown KV with this was a little less than with the smooth edged plane. This is due to the concentration of the field around the bottom electrode.

#### Point to 1 3/4" diameter plane

The breakdown curves for this electrode system are shown in Figure X, the field plot in Figure III, and corona bursts in Figure XVIII-C for  $C_3F_8$  and in Figure XVIII-D for air.

With this electrode system, final breakdown potentials depend upon the fields in the mid-gap region and this is strongly influenced by space charge distortion of the field by corona discharge.

In this system, space charge localization is more effective than with any other electrodes. Space charge will be near the point. If one increases the diameter of the point, more space charge will be there. By looking at the field map of the electrode system, one can observe that the field near the tip of the point is highly stressed. The curve for  $C_3F_8$  has more slope than for air. For air, the slope is constant throughout the plot.



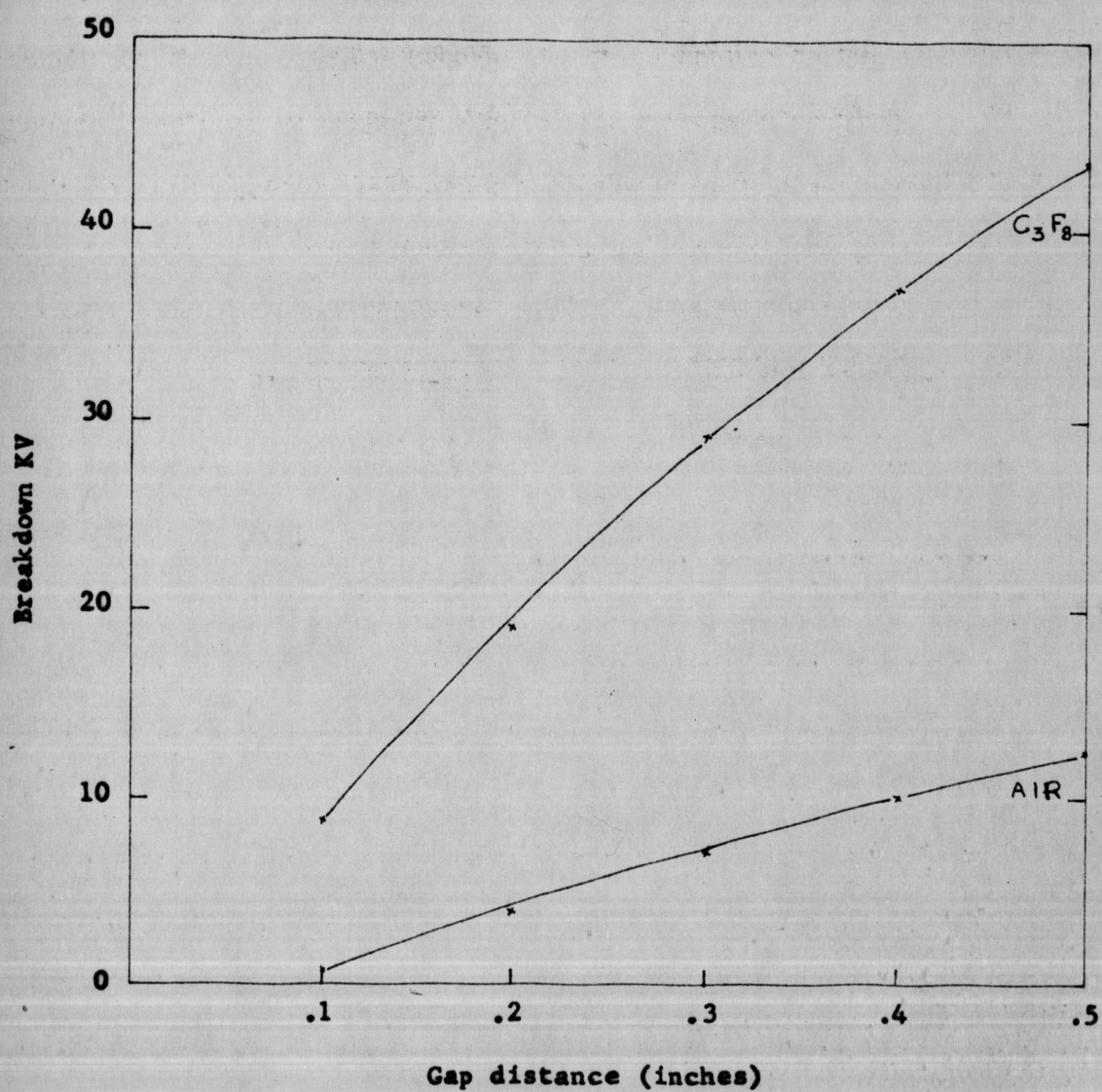


Figure X. Breakdown strengths of  $C_3F_8$  and air with the point to plane electrode system

For short gaps in air, spark breakdown occurs before stable corona is established as the field is never low enough to prevent streamer propagation across the whole gap. At 90% breakdown KV of 0.5" gap distance for this electrode system, a few corona bursts were observed for air when compared to  $C_2F_8$ .

At 90% of breakdown KV for  $C_2F_8$ , the burst pulses are very large as one can see in Figure XVIII-C. This is due to the field distortion at the tip of the point. Corona bursts started at 65% of breakdown KV.

Several investigators indicated that visual examination of the corona in air for this system shows the burst corona is associated with a brilliant blue glow near the point and the pulses are due to streamers of approximately 0.3 to 2 cm in length which often progress in a straight line to the plate. The streamers disappear as the voltage increases beyond the onset voltage and only burst corona is observed.

If one were to plot voltage current characteristics for positive point corona (d-c), one would observe that positive point current varies with voltage. First, the current increases steadily above a certain value, say  $i_0$ , which is the initial current due to external ionization. At some certain voltage, say  $V_g$ , there will be a sudden increase in current which can be observed in an oscilloscope, like pulses of current composed of small bursts of charges (approximately  $10^7$  ions), lasting approximately  $10^{-5}$  seconds until a certain value of voltage  $V_g$ . This form of corona is named by Loeb as burst corona or burst pulses as explained before. For fine points, the current will increase until the voltage reaches  $V_g$  when the corona becomes self-sustaining and external

irradiation becomes unnecessary.

For air, it is necessary, for corona to be observed, that  $E/p$  should be sufficiently high to avoid attachment over a distance of 0.1 mm from the point. Free electrons can then give rise to Townsend's avalanches directed towards the point.

### Point to point

Figure XI shows the breakdown curves of the point to point electrode system, the field plot is shown in Figure IV, and corona bursts in Figure XIX-A for  $C_3F_8$ . Breakdown KV for this electrode system has less value than any other electrode system. The field is concentrated at the two points. At these points, the field is highly stressed. The volume occupied by the gas in the gap region is very, very low when compared to the other systems.

For this electrode system, breakdown and corona bursts are nearly simultaneous in air so the picture of the bursts could not be taken. The curves for this system in  $C_3F_8$  and air are linearly proportional, since the top and the bottom electrodes are identical. Corona bursts for  $C_3F_8$  started at 7 KV, the breakdown KV is 39. In this, the corona bursts were spread in the volume occupied by the point to point. The same was observed in the oscilloscope.

### 1" diameter sphere to 1" square plane, superimposed on a 1 3/4" diameter plate

The breakdown curves for this system are shown in Figure XII, the field plot in Figure V, and the corona bursts in Figure XIX-B for  $C_3F_8$  and in Figure XIX-C for air. This system has the highest breakdown KV



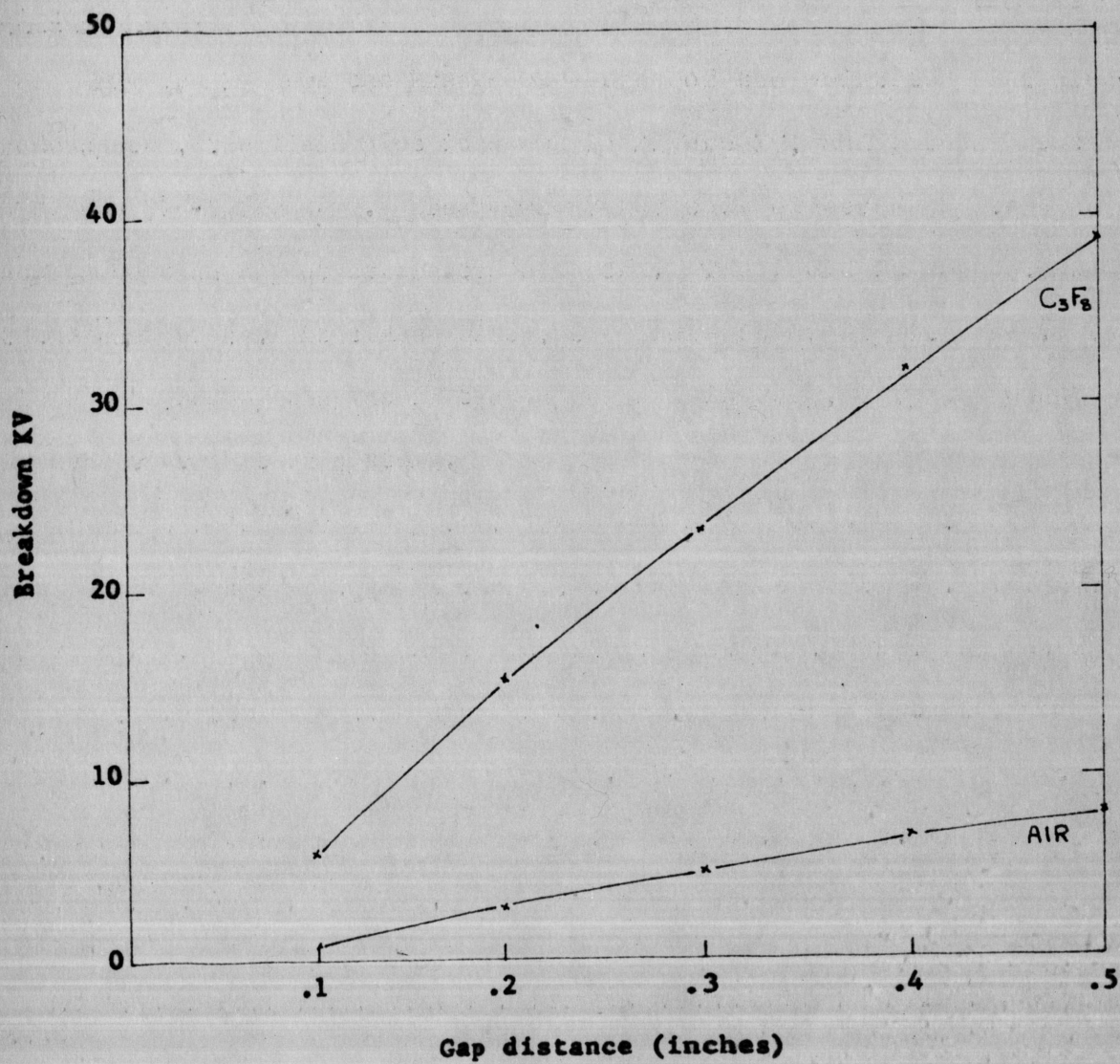


Figure XI. Breakdown strengths of  $C_3F_8$  and air with the point to point electrode system

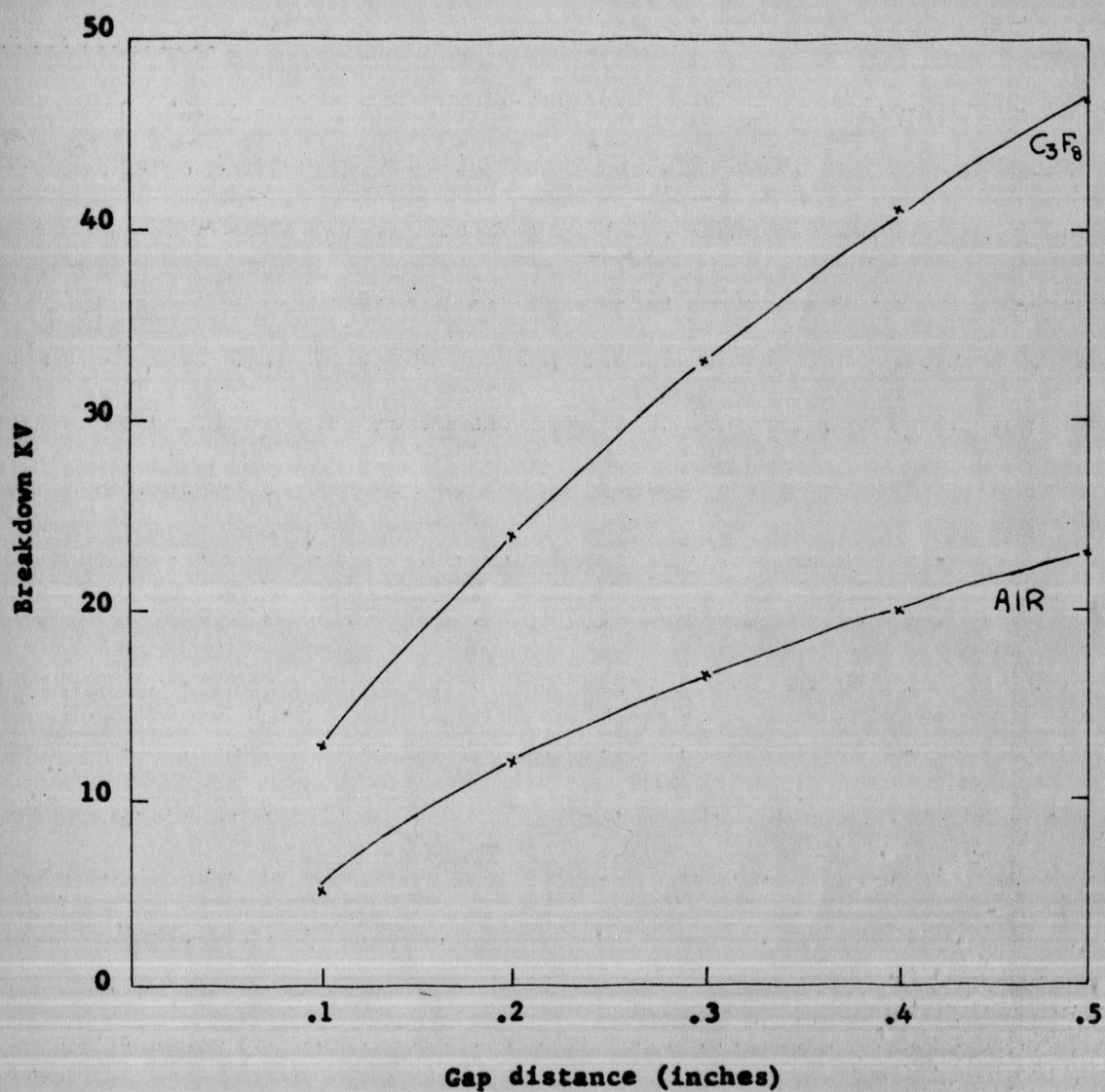


Figure XII. Breakdown strengths of C<sub>3</sub>F<sub>8</sub> and air with the sphere to square plane, superimposed on a circular plane electrode system



in  $C_3F_8$  as well as in air from 0.1" to 0.5" gap distance. The field is nonuniform at the bottom electrode. The top electrode is smaller in size. Breakdown voltage has the effect of square plate and circular plate. The field will be distributed at the square plate and the circular plate. Since the top electrode is smaller, initiation of corona starts from that electrode. The points at the bottom electrode does not have much effect on corona bursts. Corona bursts were low as one can expect. For this electrode system at 90% breakdown KV, the picture of corona bursts in air was also taken. The bursts were few as the streamers were more. Finally, spark breakdown occurred before corona was established in the whole gap.

#### 3/4" square plane to 3/4" square plane

Tests were conducted with both types of systems, that is for crossed and uncrossed electrode systems. The breakdown curves for these are shown in Figures XIII and XIV, respectively. In both cases, the curves for  $C_3F_8$  has very high slope and the curves are convex in contrast with the other systems. The field diagrams are shown in Figures VI and VII. The field is concentrated near the corners as one can observe in the field plots. Breakdown characteristics for  $C_3F_8$  can be explained as follows: Breakdown voltage depends upon the ionization of the neutral gas molecules. The positive ions which result from the ionization create a space charge field. Increasing the gap distance, increases the diffusion of positive ions, thus decreasing the space charge field which tends to retard the progress of the streamer. Therefore, at large gap distances, the decreasing of space

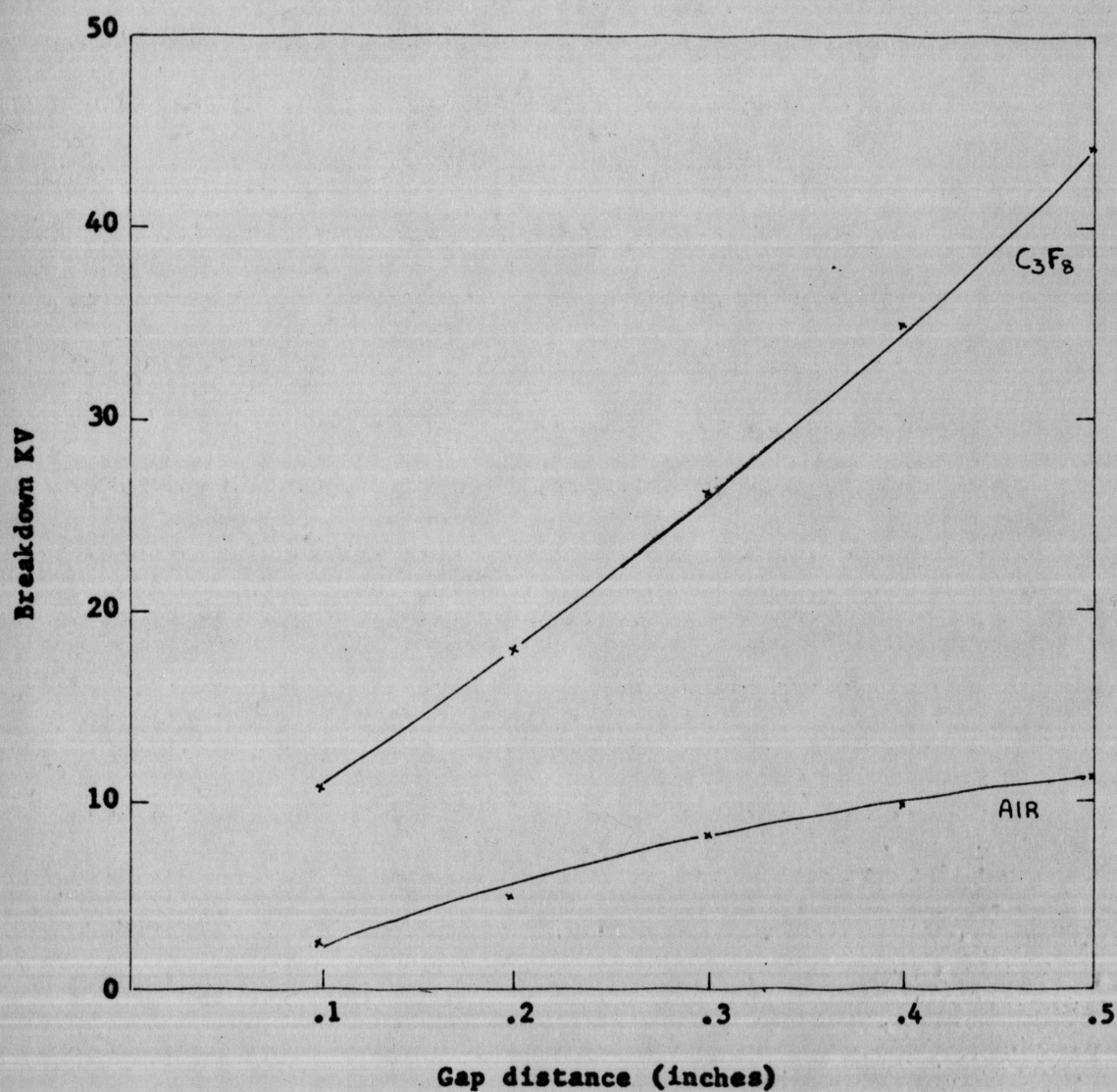


Figure XIII. Breakdown strengths of  $C_3F_8$  and air with square plane to square plane (uncrossed) electrode system



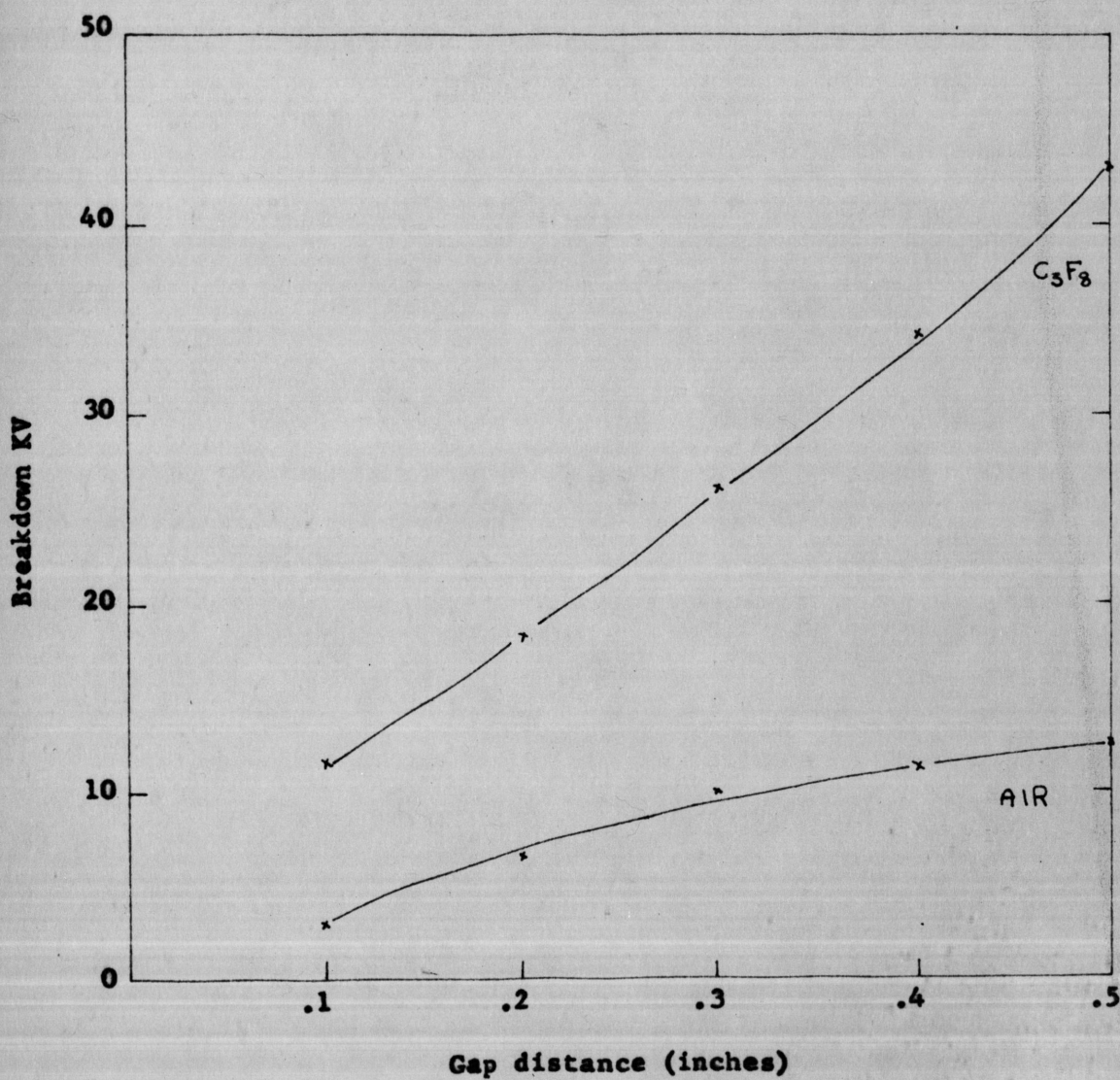


Figure XIV. Breakdown strengths of  $C_3F_8$  and air with square plane to square plane (crossed) electrode system

charge field by the diffusion of positive ions requires that a higher voltage has to be applied for the breakdown. With one square turned  $45^\circ$ , the breakdown voltage is a little less as compared to the uncrossed electrode system, since the field is nonuniform in the first case.

Corona bursts are shown for  $C_3F_8$  at 90% breakdown KV in Figure XIX-D (uncrossed system) and Figure XX-A (crossed system). In comparing both systems, there is very little difference in corona bursts. Corona bursts and spark breakdown are nearly simultaneous in air as the field is never low enough to prevent streamer propagation across the whole gap.

#### 1/2" square plane to 1 3/4" diameter plane

The breakdown curves for this electrode system are shown in Figure XV and the field plot is shown in Figure VIII. The breakdown curve of  $C_3F_8$  has a large slope. At 0.5" gap distance, breakdown value is a little less than the sphere to square plane, superimposed on a circular plane. There is field concentration near the corners. For this system, oscillographic pictures of corona bursts at 90% of breakdown KV were taken at each gap setting. They are shown for  $C_3F_8$  in Figures XX-B, C, D; XXI-A, B; and for air in Figures XXI-C, D; and in XXII-A. By studying these pictures, one can see the steady increase of corona bursts from 0.1" to 0.5" gap distances at intervals of 0.1". When the gap distance is less, streamers will be predominant. Before corona bursts become larger, spark breakdown will occur. As the gap distance increases, corona breakdown KV also increases gradually.

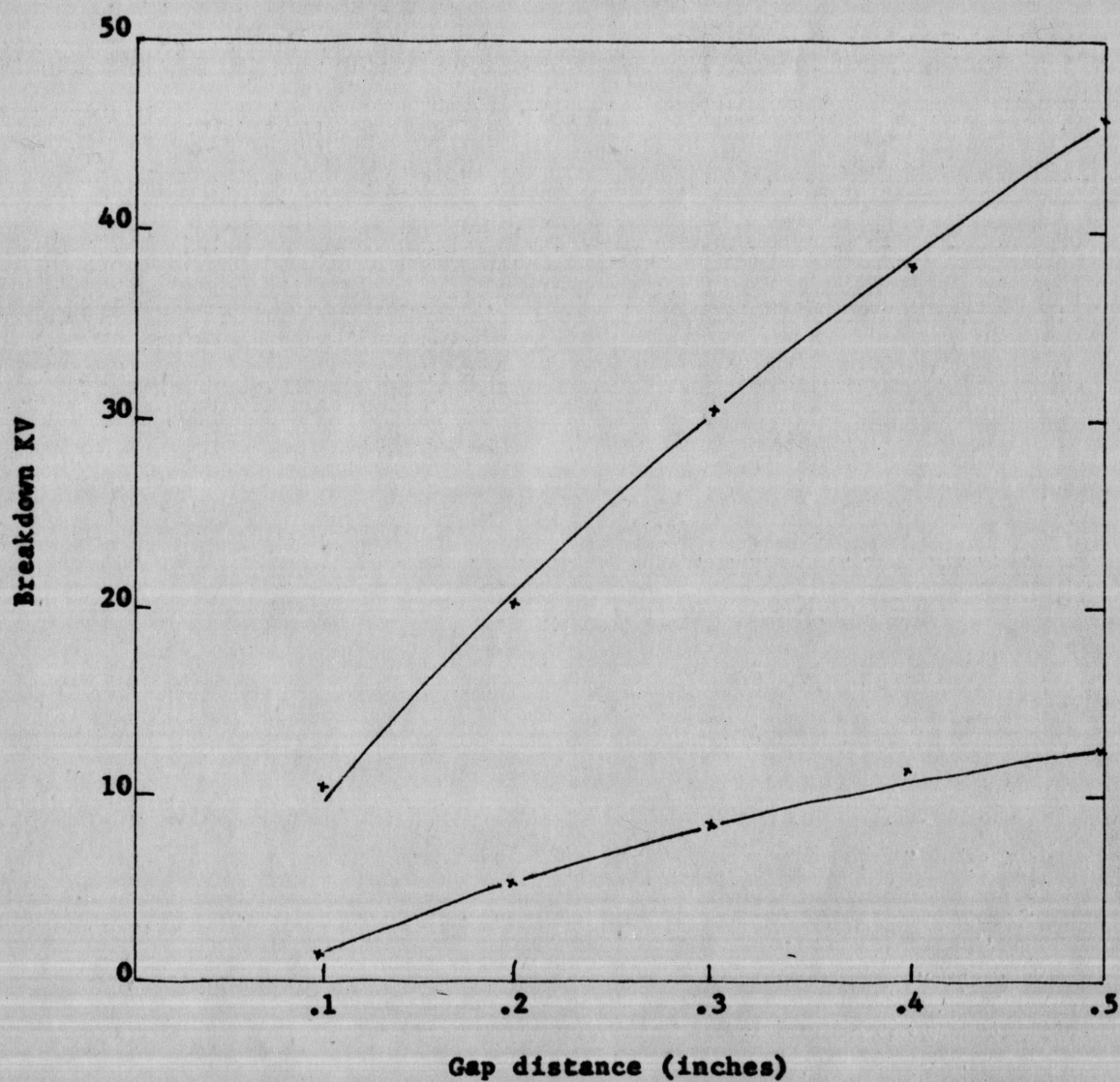


Figure XV. Breakdown strengths of  $C_3F_8$  and air with square plane to circular plane electrode system



Bursts will be more at high fields, that is one of the conditions in the theory, and as the gap distance increases, there will be time also for the bursts to become larger. Thus one can justify, as the gap distance increases, the bursts are getting larger. For air at gap distances of 0.1" and 0.2", the spark breakdown and corona are nearly simultaneous so the pictures were not taken. In this case, one can also observe the gradual increase of corona bursts as the gap distance increases, even though the bursts are very low.

#### Comparison of discharges with various types of electrode systems

Sphere to plane electrode systems and sphere to square plane, superimposed on a circular plate, have highest breakdown at low gap spacings, due to uniformity of the field and the smoothness of the electrodes. For  $C_3F_8$ , one can observe from Figure XVI that the breakdown voltages are more; for example, for the square to plane than for sphere to plane at a gap distance of 0.5". At large spacings, the curves of all the pointed electrode systems will cross the curve of the sphere to plane system. This will occur in air at very large spacings. The curves for air are shown in Figure XVII.

This is explained by Camilli, Liao, and Plump in their paper as follows: For example, for square to plane, at small spacings, negative ions formed at the square during negative voltage crest would be swept into the plane before the following positive half cycle. This breakdown can be initiated by a positive streamer. At large spacings, negative ions formed during the negative half cycle do not have time to be swept out completely and return to the plane during the positive half

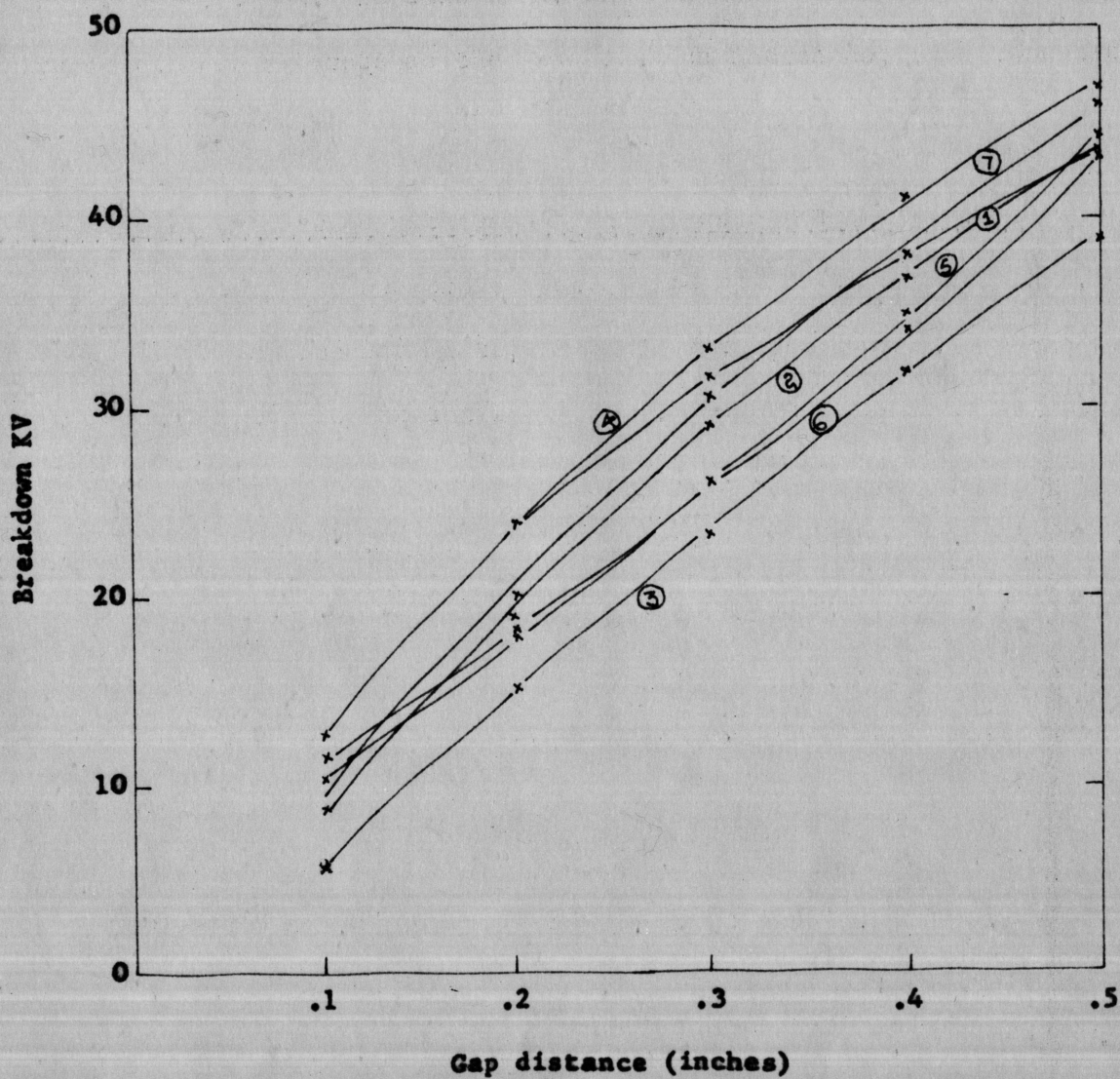


Figure XVI. Comparative study of breakdown strength of  $C_2F_8$  with the electrode systems: 1. sphere to plane, 2. point to plane, 3. point to point, 4. sphere to square plane, superimposed on a circular plane, 5. square plane to square plane (uncrossed), 6. square plane to square plane (crossed), 7. square plane to circular plane



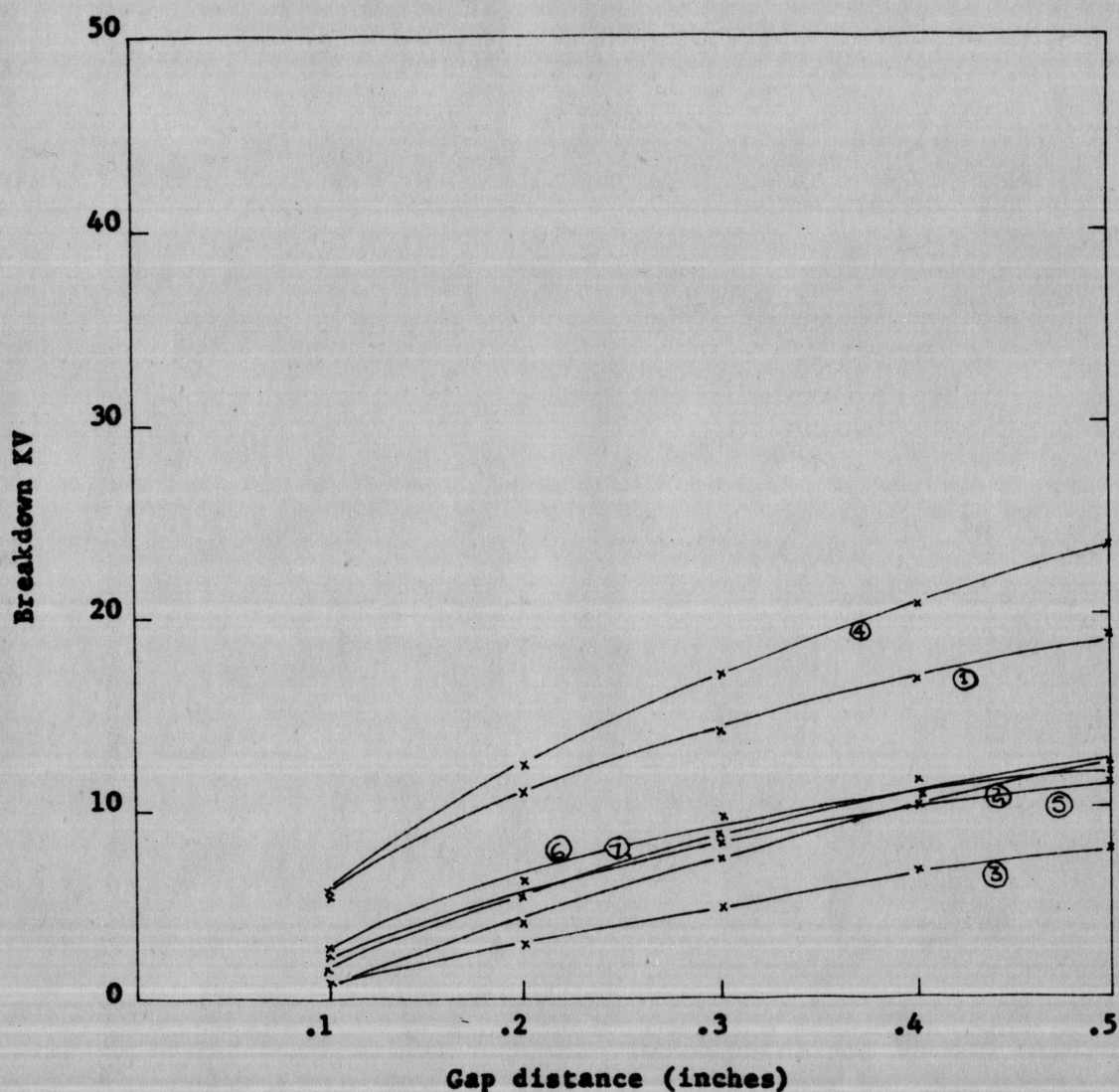
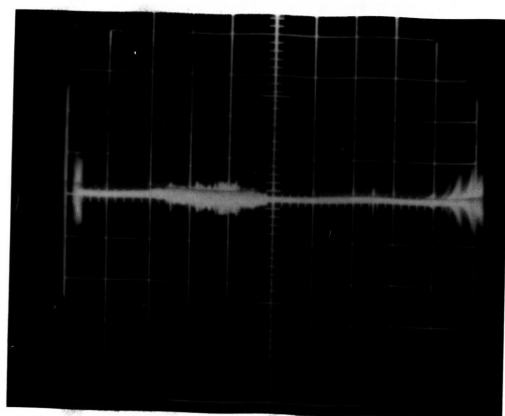


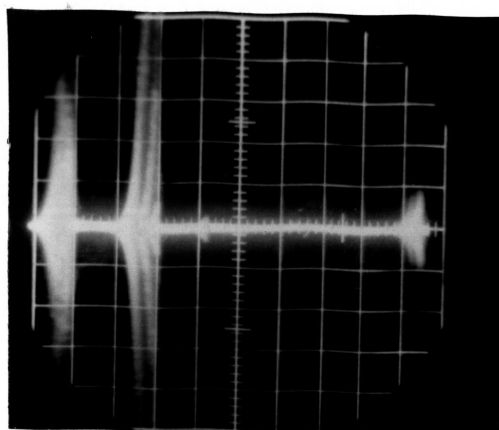
Figure XVII. Comparative study of breakdown strength of air with the electrode systems: 1. sphere to plane, 2. point to plane, 3. point to point, 4. sphere to square plane, superimposed on a circular plane, 5. square plane to square plane (uncrossed), 6. square plane to square plane (crossed), 7. square plane to circular plane

cycle. They tend to neutralize any positive ions created by positive streamer evacuating from the square, thus prohibiting the propagation of the streamer to the plane. Therefore, at large gap spacings, the square to plane breakdown values are larger than round edged electrode systems. The same reasoning can be given for other electrode systems also. For the point to point electrode system, the gap volume is so low, the breakdown voltage will not be larger than the sphere to plane until the gap spacing is very, very large when compared to the other systems.

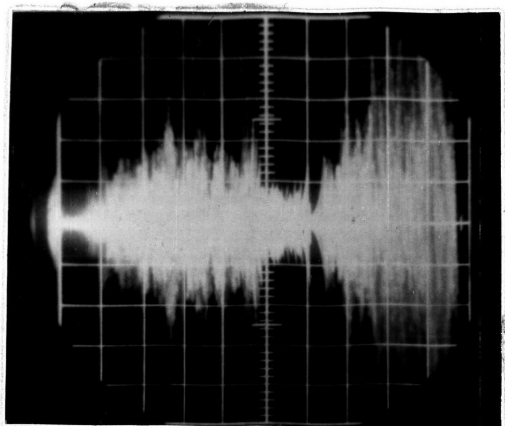
On point to plane and square to plane, larger corona bursts were observed. The point to point electrode system has less than the point to plane and square to plane, even though the field is concentrated between the two points. This can be justified as streamers are predominant and, before corona bursts become larger, spark breakdown occurs. Corona bursts are low for identical electrode systems. For sphere to plane, corona bursts are very low when compared to the other systems, as can be expected.



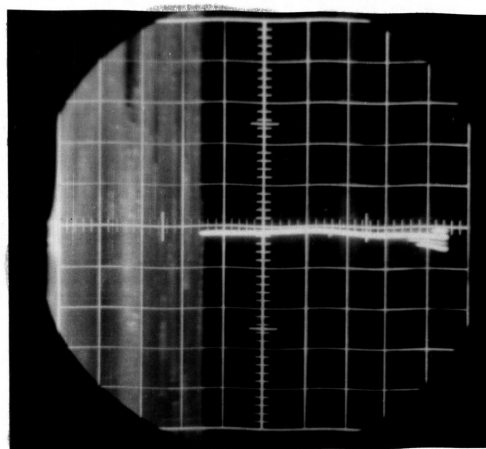
A



B



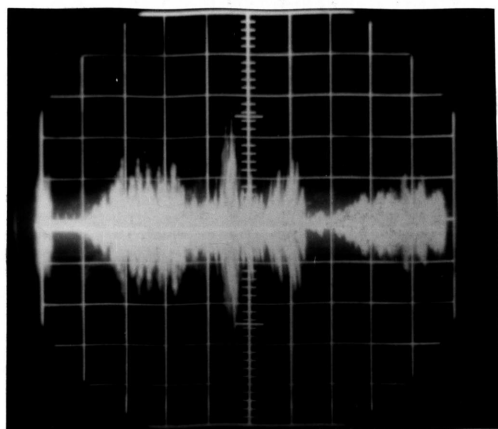
C



D

**Figure XVIII. Pictures of the corona bursts observed on the oscilloscope with the following in the test cell**

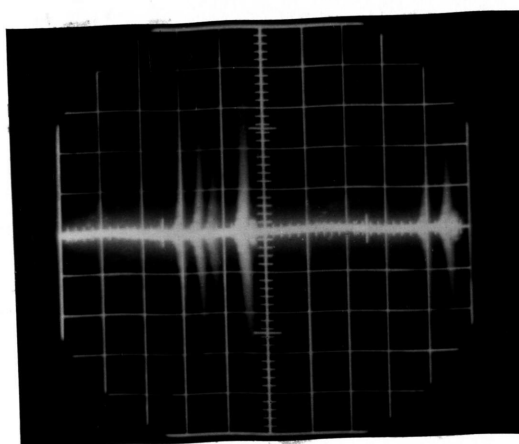
- A -  $C_2F_8$  with the sphere to plane electrode system**
- B - Air with the sphere to plane electrode system**
- C -  $C_2F_8$  with the point to plane electrode system**
- D - Air with the point to plane electrode system**



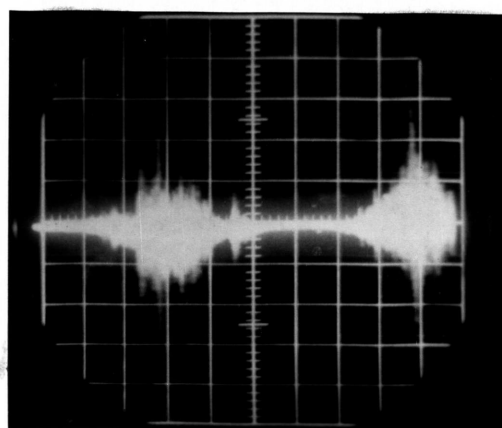
A



B



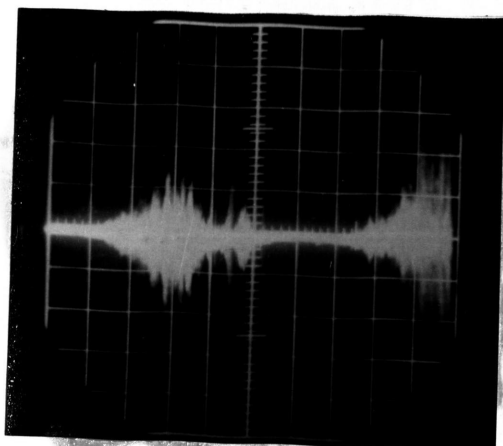
C



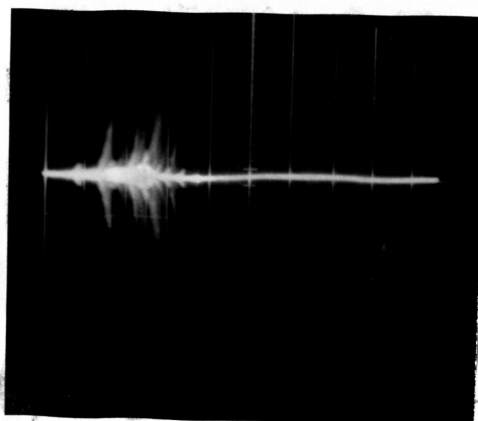
D

Figure XIX. Pictures of the corona bursts observed on the oscilloscope with the following in the test cell

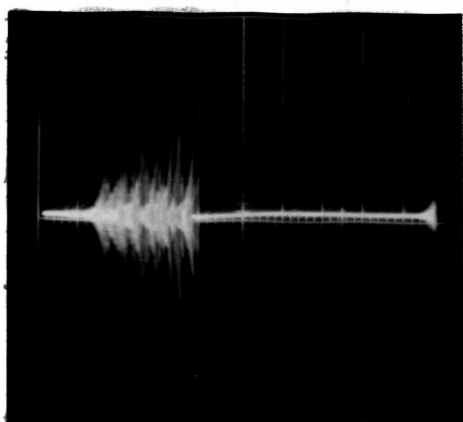
- A -  $C_3F_8$  with the point to point electrode system
- B -  $C_3F_8$  with the sphere to square plane, superimposed on a circular plane electrode system
- C - Air with the sphere to square plane, superimposed on a circular plane electrode system
- D -  $C_3F_8$  with the square plane to square plane (uncrossed) electrode system



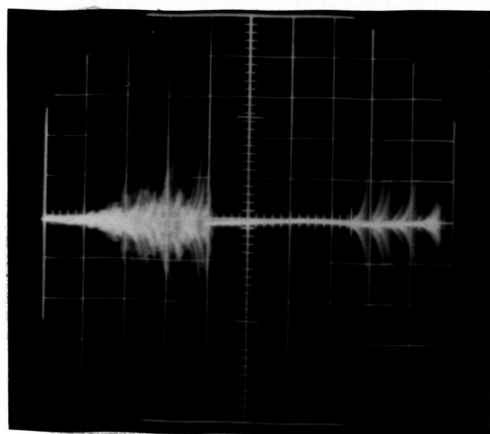
A



B



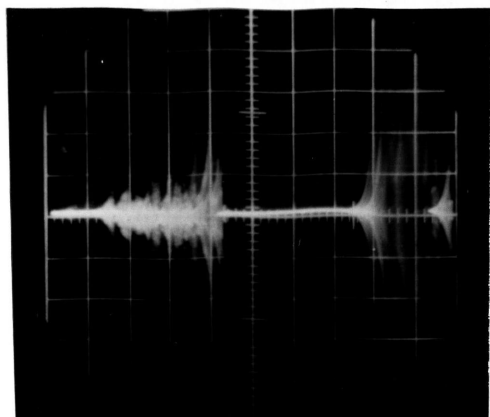
C



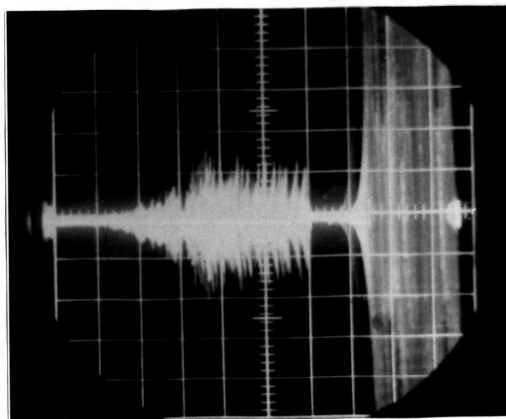
D

Figure XK. Pictures of the corona bursts observed on the oscilloscope with the following in the test cell

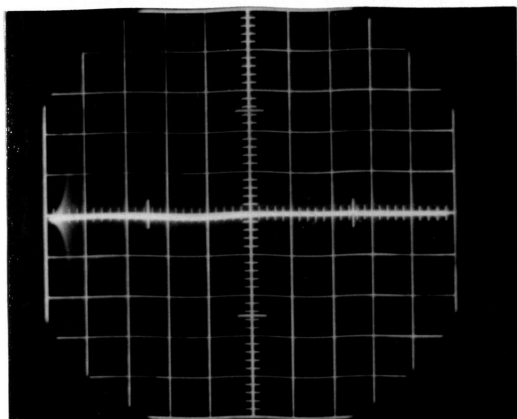
- A -  $C_3F_8$  with the square plane to square plane (crossed) electrode system
- B -  $C_3F_8$  with the square plane to circular plane electrode system with gap distance of 0.1"
- C -  $C_3F_8$  with the square plane to circular plane electrode system with gap distance of 0.2"
- D -  $C_3F_8$  with the square plane to circular plane electrode system with gap distance of 0.3"



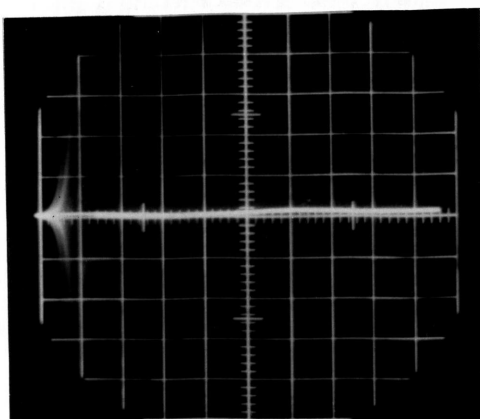
A



B



C



D

Figure XXI. Pictures of the corona bursts observed on the oscilloscope with the following in the test cell

- A -  $C_3F_8$  with the square plane to circular plane electrode system with gap distance of 0.4"
- B -  $C_3F_8$  with the square plane to circular plane electrode system with gap distance of 0.5"
- C - Air with the square plane to circular plane electrode system with gap distance of 0.3"
- D - Air with the square plane to circular plane electrode system with gap distance of 0.4"



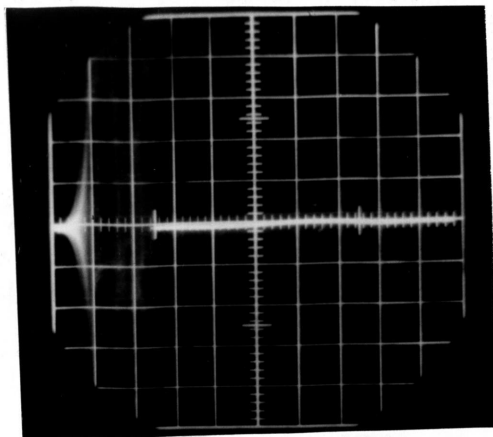


**Figure XXII. Picture of the corona bursts observed on the oscilloscope with the following in the test cell**

**Air with the square plane to circular plane  
electrode system with gap distance of 0.5"**

## CHAPTER VI

## CONCLUSIONS

The investigations lead the author to the conclusions which are listed as follows:

1.  $C_3F_8$  has high dielectric strength due to the property of electronegativity of the gas.
2. Air has low dielectric strength. Air contains a large percentage of nitrogen. The negative ions of nitrogen are extremely unstable or nonexistent. Due to this property and the mixture property of air, the breakdown KV of air is less than  $C_3F_8$ .
3. At low gap spacings, round edged electrode systems have high dielectric strength.
4. At large gap spacings, pointed electrode systems have higher breakdown strengths than the round edged systems.
5. Field plotting is found to be one of the best ways to understand the configuration of the electrode systems.
6. Field near the points is highly stressed.
7. For two identical square planes, there is little difference in breakdown KV when the two planes are crossed or when uncrossed, indicating the distortion of the field.
8. With square to plane electrode systems, largest corona bursts were observed.
9. At 0.5" gap spacings, a 1" diameter sphere to 1" square plane, superimposed on a circular plate electrode system, has the highest breakdown strength of all systems used.
10. For pointed electrode systems in air, the breakdown KV is very low. Spark breakdown and corona bursts are nearly simultaneous.
11. Roughness and cleanliness of the electrode system effect the breakdown KV.
12.  $C_3F_8$  can be used as a dielectric for its high breakdown strength over other gases and the only disadvantage of  $C_3F_8$  is that when the breakdown occurs, one can observe small deposits of carbon on the electrode of the systems.

## LITERATURE CITED

- Berberich, L. J., Works, C. N., and Lindsay, N. W., "Electric Breakdown of Perfluorocarbon Vapours and Their Mixtures with Nitrogen", AIEE Transactions, vol. 74, 1955, pt. 1, pp. 660-666.
- Camilli, G. and Chapman, J. J., "Gaseous Insulation for High Voltage Apparatus", AIEE Transactions, vol. 66, 1947, pp. 1463-1470.
- Camilli, G., Liao, T. W., and Plump, R. E., "Dielectric Behaviour of Some Fluorogases and Their Mixtures", AIEE Transactions, vol. 74, 1955, pt. 1, pp. 634-642.
- Camilli, G. and Plump, R. E., "Fluorine Containing Gaseous Dielectrics", AIEE Transactions, vol. 72, 1953, pt. 1, pp. 93-102.
- Cobine, J. D., "Some Electrical and Thermal Characteristics of Helium and Sulphur Hexafluoride Mixtures", AIEE Transactions, vol. 74, 1955, pt. 1, pp. 318-321.
- Fitzsimmons, R. E., "Threshold Field Studies of Various Positive Corona Phenomenon", Physical Review, vol. 61, 1942, pp. 175-182.
- Kip, Arthur F., "Positive Point-to-Plane Discharge in Air at Atmospheric Pressure", Physical Review, vol. 54, 1938, pp. 138-146.
- Kip, Arthur F., "Onset Studies of Positive Point-to-Plane Corona in Air at Atmospheric Pressure", Physical Review, vol. 55, 1939, pp. 549-556.
- Loeb, Leonard B., Fundamental Processes of Electrical Discharge in Gases, John Wiley & Sons, Inc.: New York, New York, 1939.
- Loeb, Leonard B. and Meek, John M., The Mechanism of the Electric Spark, Stanford University Press: California, 1941.
- Manning, M. L., "Experience With the AIEE Subcommittee Test Cell for Gaseous Insulation", AIEE Transactions, vol. 78, 1959, pt. 3, pp. 800-807.
- Meek, J. M., "A Theory of Spark Discharge", Physical Review, vol. 57, 1940, pp. 722-728.
- Moore, A. D., "Mapping Techniques Applied to Fluid Mapper Patterns", AIEE Transactions, vol. 71, 1952.
- Pollock, H. C. and Cooper, F. S., "The Effect of Pressure on the Positive Point to Plane Discharge in  $N_2$ ,  $O_2$ ,  $CO_2$ ,  $SO_2$ ,  $SF_6$ ,  $CCl_2F_2$ , A, He, and  $H_2$ ", Physical Review, vol. 56, 1939, pp. 170-175.

Trichel, G. W., "The Mechanism of the Negative Point to Plane Corona Near Onset", Physical Review, vol. 54, 1938, pp. 1078-1084.

Trichel, G. W., "The Mechanism of the Positive Point to Plane Corona in Air at Atmospheric Pressure", Physical Review, vol. 55, 1939, pp. 382-390.

Works, C. H. and Dakin, T. W., "Dielectric Breakdown of  $\text{SF}_6$  in Nonuniform Fields", AIEE Transactions, vol. 72, 1953, pt. 1, pp. 682-687.